Trends and variability in the ocean carbon sink

Gruber Nicolas [1, *], Bakker Dorothee C. E. [2], Devries Tim [3, 4], Gregor Luke [1], Hauck Judith [5], Landschützer Peter [6, 7], McKinley Galen A. [8, 9], Müller Jens Daniel [1]

[1] Environmental Physics, Institute of Biogeochemistry and Pollutant Dynamics, ETH Zurich, Zürich, Switzerland
[2] Centre for Ocean and Atmospheric Sciences, School of Environmental Sciences, University of East Anglia, Norwich, UK
[3] Department of Geography, University of California, Santa Barbara, CA, USA
[4] Earth Research Institute, University of California, Santa Barbara, CA, USA
[5] Alfred-Wegener-Institut, Helmholtz-Zentrum für Polar und Meeresforschung, Bremerhaven, Germany
[6] The Ocean in the Earth System, Max Planck Institute for Meteorology, Hamburg, Germany
[7] Department Research, Flanders Marine Institute (VLIZ), Ostend, Belgium
[8] Department of Earth and Environmental Sciences, Columbia University, New York, NY, USA
[9] Lamont Doherty Earth Observatory, Palisades, NY, USA

* Corresponding author : Nicolas Gruber, email address : nicolas.gruber@env.ethz.ch

Abstract :

The ocean has absorbed 25 ± 2% of the total anthropogenic CO2 emissions from the early 1960s to the late 2010s, with rates more than tripling over this period and with a mean uptake of –2.7 ± 0.3 Pg C year–1 for the period 1990 through 2019. This growth of the ocean sink matches expectations based on the increase in atmospheric CO2, but research has shown that the sink is more variable than long assumed. In this Review, we discuss trends and variations in the ocean carbon sink. The sink stagnated during the 1990s with rates hovering around –2 Pg C year–1, but strengthened again after approximately 2000, taking up around –3 Pg C year–1 for 2010–2019. The most conspicuous changes in uptake occurred in the high latitudes, especially the Southern Ocean. These variations are caused by changes in weather and climate, but a volcanic eruption-induced reduction in the atmospheric CO2 growth rate and the associated global cooling contributed as well. Understanding the variability of the ocean carbon sink is crucial for policy making and projecting its future evolution, especially in the context of the UN Framework Convention on Climate Change stocktaking activities and the deployment of CO2 removal methods. This goal will require a global-level effort to sustain and expand the current observational networks and to better integrate these observations with models.

Key points

i) The long-term trend in the ocean carbon sink since the early 1960s was primarily driven by the increasing uptake of anthropogenic CO_2. Although the ocean is expected to have lost a few petagrams of natural CO_2 to the atmosphere in response to ocean warming, this loss cannot be quantified conclusively with observations.

ii) The oceanic uptake of anthropogenic CO_2 scaled proportionally with the increase in atmospheric CO_2 between the early 1960s and late 2010s, as expected given the quasi-exponential growth of atmospheric CO_2 during this period.

iii) The average ocean uptake rate of -2.7 ± 0.2 Pg C yr^{-1} for the period 1990 through 2019 yields a proportionality β of 1.4 ± 0.1 Pg C per ppm of atmospheric CO_2, suggesting a trend in the uptake of -0.4 ± 0.1 Pg C yr^{-1} decade^{-1}.

iv) The ocean carbon sink varies by about $\pm20\%$ around this trend, primarily caused by changes in the sources and sinks of natural CO_2, with a lesser role for variations in atmospheric CO_2 growth rates impacting the uptake of anthropogenic CO_2.

v) The net oceanic uptake rate of CO_2 will likely decrease in the future owing to several converging trends: reduced emissions of CO_2 leading to reduced atmospheric CO_2 growth rates in response to climate policy; reduced storage capacity owing to continuing ocean acidification; and enhanced outgassing of natural CO_2 owing to ocean warming and changes in ocean circulation and biology.

62   **[H1] Introduction**

63

64   Throughout the Anthropocene, the ocean has been the largest and most persistent sink for the anthropogenic

65   CO_2 emitted into the atmosphere by the burning of fossil fuels, cement production, and land use change [1–4].

66   This importance was recognized already by the late 19th century[5,6], with the chemist Arrhenius[7] estimating

67   that about 83% of the emitted anthropogenic CO_2 would be taken up by the ocean. Therefore, he concluded

68   that no noticeable global warming should be expected from the emissions of anthropogenic CO_2, since the

69   uptake by the ocean uptake leave only a small fraction of the emissions accumulating in the atmosphere.

70   Although his estimate of the long-term capacity of ocean uptake was accurate[8,9], Arrhenius was not aware

71   that it takes thousands of years for the ocean to fully realize this capacity and not decades as he implicitly

72   assumed[6]. Arrhenius' view was widely shared, so that the scientific community was oblivious to the growing

73   threat from the CO_2 emissions that were increasing by several percent per year for most of the early 20th

74   century [10]. Revelle and Suess[11] realized this mistake in 1957. Thereafter, the perspective of the scientific

75   community on the issue of human-induced climate change shifted rapidly[12,13], especially after Keeling

76   confirmed in 1960 that atmospheric CO_2 was increasing much more rapidly than implied by Arrhenius[14].

77   Much of global ocean carbon cycle research since Revelle and Suess' discovery has focused on quantifying

78   the fraction of the CO_2 emissions taken up by the ocean, and to understand the processes that limit this

79   uptake, preventing the ocean from reaching the huge capacity of more than 80% that Arrhenius had

80   identified. A crucial step to address this question was the conceptualization of the net exchange of CO_2 across

81   the air-sea interface and the change in the stock of dissolved inorganic carbon (DIC) [G] to consist of two

82   components: anthropogenic CO_2 and natural CO_2 (Box 1). The anthropogenic CO_2 component, previously

83   often referred to as excess CO_2 [15], can be considered the perturbation component, as it is solely a consequence

84   of the anthropogenic increase in atmospheric CO_2. The natural CO_2 component of the flux is associated with

85   the pre-industrial pool of DIC in the ocean (order of 37,000 Pg C (1 Pg 10^{15}g) [16] and is involved in air-sea gas

86   exchange [G] , uptake and release by the biological pumps, interactions with and loss to the sediments, and

87   input by rivers (Box 1).

88   Under the assumption of a steady-state ocean, which is supported by the relative constancy of climate and

89   atmospheric CO_2 for centuries prior to the onset of the industrial revolution (~1800)[17], the oceanic pool of

90   natural CO_2 remains constant and the fluxes of natural CO_2 are globally balanced. This assumption permitted

91   researchers already in the 1970s to use models and observations to determine the oceanic uptake of

92   anthropogenic CO_2 [18–20], with subsequent work refining the methods and improving the data base [2,4,15,21,22].

93   However, it has become increasingly clear since the 2000s that the natural carbon fluxes of the ocean are

94   changing, and that the ocean sink for carbon is more variable[23–32]. The natural CO_2 pool is in fact highly

95   mobile, responding to changes in physical forcing from the atmosphere through changes in winds and in the

96   fluxes of heat and freshwater, inducing changes in ocean circulation, temperature, salinity, and ocean

97   biology[9]. Moreover, the anthropogenic CO_2 pool is more changeable than previously thought, responding to

98   changes in atmospheric CO_2 growth rate or changes in ocean circulation[33].

99   In this Review, we assess what is currently known about the ocean sink for CO_2, and how it has responded to

100 the rising CO_2 emissions in recent decades, relying primarily on ocean observations. We describe the

101 variability of this sink and its drivers, which are debated. Finally, we highlight the need for increased

102 observational capacity to support long term decision making, especially for the use of oceanic carbon dioxide

103 removal (negative emission) approaches.

104

105 **[H1] OCEAN CARBON SINK TRENDS**
106

107 Since the late 1950s, the ocean has taken up a net $25 \pm 2\%$ of the total anthropogenic CO_2 emissions[1]. This

108 fractional uptake has remained relatively constant through time, meaning that the ocean sink tripled over

109 these six decades, increasing from about -0.9 Pg C yr^{-1} in the early 1960s to more than -3 Pg C yr^{-1} in 2020[1,25]

110 (note that the geophysical convention of fluxes being are considered positive here, so that an uptake of CO_2 is

111 negative). This increasing ocean carbon sink is an ecosystem service that amounts to about 2 trillion Euros

112 worth of emission reductions per year if valued at a typical marginal abatement cost compatible with a 1.5°C

113 target of 200 Euro per ton of CO_2 [34]. Together with the large ocean uptake of the excess heat generated from

114 rising atmospheric CO_2[35], the ocean has moderated the climate change experienced so far[36,37]. This section

115 reviews how this ocean sink has been determined and what drives this long-term trend.

116

117

118 *[H2] Response to rising atmospheric CO_2*

119 The primary driver causing a long-term (> decades) change in the ocean's inventory of DIC is the rise in

120 atmospheric CO_2, driving a flux of anthropogenic CO_2 across the air-sea interface and then from the surface

121 ocean to depth (Box 1). The rate limiting step for the uptake of anthropogenic CO_2 by the ocean is the

122 transport from the surface to deeper layers [38], as it takes decades to centuries for waters to circulate from the

123 surface to the deeper ocean and back again[39,40]. In contrast, CO_2 gas exchange across the air-sea interface is

124 comparably fast (e-folding time scale of less than a year[9,41]), so that the CO_2 concentration of the surface

125 ocean follows the atmospheric perturbation relatively closely[42–44], with the magnitude of increase determined

126 by the surface ocean's buffer (or Revelle) factor[9,45,46] **[G]**. The two processes air-sea exchange and the

127 surface-to-deep transport of CO_2 respond approximately linearly to changes in atmospheric CO_2. However,

128 there is some the moderate non-linearity owing to the ocean's decreasing buffering capacity due to ocean

129   acidification [G] (a decrease of about 10% since preindustrial times[47]) that needs to be taken into account as

130   well [48,49].

131   When a (near)linear system like the ocean uptake of anthropogenic CO_2 (C_{ant}) is forced exponentially with a

132   fixed growth rate (as is the case for atmospheric CO_2 since ~1970) (Fig 1a), all components of the system will

133   increase proportionally after an initial adjustment (which is about a decade[50]). This proportionality implies a

134   linear scaling between the forcing (atmospheric CO_2) and the response (ocean accumulation of anthropogenic

135   CO_2), which is confirmed by results from observations[2,4], ocean inverse models[3] [G] and forward simulations

136   [G] with ocean biogeochemical models[25,51] [G] (Fig 1a). The slope of this relationship (the line in Fig 1a)

137   represents the carbon concentration feedback of the ocean [52,53] and is described as the sensitivity, where β =

138     $\partial C_{ant} / \partial \Delta CO_2{}^a$, with the exact value dependent on the forcing history and especially past atmospheric growth

139   rate. An emergent property of this relationship is that during periods of exponential growth in atmospheric

140   CO_2, it directly determines the global oceanic uptake flux of anthropogenic CO_2 ($F_{ant}(t)$) from the growth rate

141   of atmospheric CO_2: $dC_{ant}/dt = -F_{ant}(t) = \beta \cdot d\Delta CO_2{}^a/dt$, where the negative sign in front of F_{ant} reflects the

142   convention of ocean uptake being negative.

143   This simple scaling relationship does not apply once the atmospheric CO_2 growth begins to deviate

144   substantially from an exponential, as is expected if emissions start to stabilize and decrease in response to

145   global efforts to curb climate change[54]. In such cases, more complete theories building on deconvolution

146   concepts such as pulse response functions [3,55] or transit time distributions (TTD) [56–58] are much better suited

147   to describe the oceanic uptake of anthropogenic CO_2[59]. Nevertheless, the high CO_2 concentration in the

148   atmosphere would still be the main driving force for the many centuries it takes to equilibrate the entire ocean

149   with the atmospheric perturbation.[60]

150

151   *[H2] Cumulative oceanic uptake*

152   The tight relationship between the ocean uptake for anthropogenic CO_2 and the growth in atmospheric CO_2

153   was recognized by the 1970s[18,61,62]. However, until the mid-1980s, high-quality measurements of oceanic DIC

154   were extremely scarce[63], making it impossible to constrain this relationship with observations. As the number

155   of reliable DIC measurements increased in the late 1970s methods to identify the anthropogenic CO_2 signal

156   within the substantial background variability of DIC emerged [19,20]. Since the data were typically available

157   only from a one-time survey, back-calculation approaches were used that implicitly assume a steady-state

158   ocean. In such approaches, the DIC concentration in a water parcel in the ocean's interior is traced back to its

159   origin at the surface, correcting along the way for the biological changes that incurred along this journey from

160   the surface to depth[15,21]. Refinement of the initial approaches led to the ΔC^* method[64,65], which is the most

161   widely used back-calculation method to identify the total amount of anthropogenic CO_2 that has accumulated

162   in the ocean since preindustrial times [21]. A crucial enabling development for the identification of the

163   relatively small anthropogenic CO_2 signal (see also Box 1) was the introduction of common measurement

164   methodologies[66] and certified reference materials[67,68] that permitted the collation of DIC measurements taken

165   years apart and measured by different laboratories around the world into an internally coherent data set [69].

166   The application of the ΔC^* approach to the data collected by the Joint Global Ocean Flux Study

167   (JGOFS)/World Ocean Circulation Experiment (WOCE) programs in the mid-1980s to mid-1990s led to the

168   first global data-based estimate of the accumulation of anthropogenic CO_2 [2]. This approach yielded a total

169   anthropogenic CO_2 inventory for the nominal year 1994 of 118 ±19 Pg C (Fig 1a), i.e., reflecting the time

170   integrated ocean uptake since ~1800. The maps in Fig 1b show the well-established spatial variations in the

171   vertically integrated amount of anthropogenic CO_2 [38,70–72] (Fig. 1b). Strong accumulation in the North Atlantic

172   contrasts with regions of relatively low accumulation such as the Tropical Pacific and the polar Southern

173   Ocean. One of the most conspicuous features of the spatial variation is the band of high accumulation north

174   of the Southern Ocean between about 30°S to 40°S. These basin-scale differences are a direct consequence of

175   the regional effectiveness with which anthropogenic CO_2 is transported from the surface downward into the

176   ocean's interior [70,72–74]. The Ocean Inversion Project used such knowledge about the surface to depth

177   transport in the form of impulse response functions, to estimate how much uptake of anthropogenic CO_2 is

178   required in order to match the reconstructed distribution of anthropogenic CO_2 in 1994. This estimate yielded

179   an uptake flux of -2.2 ± 0.25 Pg C yr^{-1} for a nominal year 1995 [72].

180   This inventory also provided the first observation-based estimate of β of 1.47±0.24 Pg C / ppm CO_2,

181   representing the time period 1800-1994 (Supplementary Table 1). These results confirmed many prior

182   estimates that so far had relied on models[18,38,71] or indirect constraints such as the changes in atmospheric

183   oxygen[75] or budgets of the stable isotope of carbon (^{13}C)[76–78].

184   ***[H2] Decadal trends in uptake***

185

186   The linear β-scaling can be used to provide a first estimate of the further evolution of the oceanic sink. Given

187   the observed trend in the atmospheric CO_2 growth rate of 0.3 ppm yr^{-1} decade^{-1} between 1994 and 2007 and

188   the inferred sensitivity β of 1.47±0.24 Pg C / ppm CO_2, one would expect the steady-state ocean sink for

189   anthropogenic CO_2 to increase (become more negative) by about -0.4 Pg C decade^{-1} over this period, yielding

190   an uptake in 2007 of the order of -2.6 Pg C yr^{-1}. Forward and inverse models[3,25,70,79] have been used to assess

191   this trend prediction (Fig 1a), but the ultimate evidence has to come from direct documentation of the

192   increase in the ocean's DIC pool.

193   Direct documentation of decadal trends in anthropogenic CO_2 uptake is not straightforward, as shorter-term

194   variations in the natural carbon pool tend to mask the slower but steadier increase in anthropogenic CO_2. This

195   problem can be overcome for regularly sampled timeseries[43,80,81], but only a few sites have sufficient

196   observations to distinguish the anthropogenic trend from the natural variability. In most cases, the sampling

197   rate is once per decade, as is the case for the GO-SHIP Global Repeat Hydrography Program[82], for example.

198   These data suffer acutely from an overprint of short-term variability in the natural carbon cycle, typically

199   leading to a very noisy pattern of change that is difficult to interpret[83].

200   The introduction of the extended multiple linear regression (eMLR) approach[84] enabled the change in

201   anthropogenic CO_2 to be mostly isolated[85,86]. This method is the most widely used approach for detecting and

202   quantifying changes in the anthropogenic CO_2 in the interior ocean based on repeat hydrography cruises[83,87–

203   89]. Compared to the ΔC^* approach, the eMLR approach captures both the steady-state and the non-steady-

204   state accumulation of anthropogenic CO_2, although with limited accuracy when reconstructing the non-

205   steady-state component[90].

206   A modified version of the eMLR method (eMLR(C*) method [90]) was used to estimate the change in

207   anthropogenic CO_2, ΔC_{ant}, globally[4], using DIC and other biogeochemical data from the JGOFS/WOCE

208   survey for the 1990s and comparing them with the measurements from the 2000s obtained during the 1st

209   round of the GO-SHIP Repeat Hydrography Program[82] (Fig. 1c). Global ocean carbon storage was estimated[4]

210   to increase by 34 ± 4 Pg C between 1994 and 2007, bringing the total inventory for anthropogenic CO_2 for

211   2007 to 154 ± 19 Pg C (Fig 1a). This increase in storage corresponds to a mean ocean uptake flux of

212   anthropogenic CO_2 of -2.6 ± 0.3 Pg C yr^{-1} over the 1994 to 2007 period, corroborating the simple scaling

213   prediction. It also suggests a sensitivity β of 1.39 ± 0.16 Pg C / ppm CO_2, which is statistically

214   indistinguishable from that estimated from the anthropogenic CO_2 inventory in 1994 (1.47 ± 0.24 Pg C / ppm

215   CO_2, Supplementary Table 1). This lack of a difference provides strong support for the steady-state

216   assumption.

217   Given this steady-state, the ocean interior estimate for 1994 to 2007 can be scaled to each decade over the

218   past 30 years using β, yielding -2.1 Pg C yr^{-1} for 1990 to 1999, -2.6 Pg C yr^{-1} for the subsequent decade, and -

219   3.3 Pg C yr^{-1} for 2010 through 2019 (Table 1). Models suggest a smaller sensitivity β, lower mean uptake and

220   smaller decadal trends (Table 1, Supplementary Table 1). However, many of the differences are not

221   statistically significant, confirming that the ocean acts as a strong and increasing sink for anthropogenic CO_2.

222   Overall, the steady-state assumption is useful determining the multidecadal oceanic uptake of anthropogenic

223   CO_2 However, this assumption does not hold as well when analyzing shorter-term variations or spatial

224   variations.

225

226   *[H2] Non-steady-state uptake*

227

228   A more detailed analysis of the spatial variations in the ocean interior accumulation of anthropogenic CO_2

229   highlights the limits of the steady-state assumption (Fig 1b,c). To first order, the increase in anthropogenic

230   CO_2 is proportional to how much anthropogenic CO_2 was present at the beginning [4,42,91]. The proportionality

231   can be estimated using the β approach, yielding a value of 0.28±0.02 for the inventory in 1994 and the change

232   in inventory[4] between 1994 and 2007 (similar approaches using a transit-time distribution (TTD) approach[57]

233   yield comparable results). Thus, differences in the scaled spatial distribution of C_{ant} (1994) (Fig 1b) and

234   ΔC_{ant}(2007-1994) (Fig 1c) suggest a non-steady-state contribution. Although the uncertainties in the two

235   reconstructions are substantial, they suggest a shift in the accumulation of anthropogenic CO_2 from the North

236   Atlantic to the South Atlantic, potentially related to decadal shifts in the overturning circulation [92]. This

237   pattern confirms the presence of substantial decadal variability in the ocean carbon cycle identified

238   previously along basin-wide hydrographic sections that had been occupied multiple times[83,89]. However, the

239   decadal nature of the repeat hydrography program limits the ability to constrain the year-to-year variability of

240   the ocean carbon sink via the changes in the carbon storage.

241

242   **[H1] OCEAN CARBON SINK VARIABILITY**
243

244   Analyses of the sea-to-air fluxes of CO_2 are better suited to address this challenge, as they can be used to

245   analyze changes at much higher temporal resolutions. In addition, they also assess the potential contribution

246   of the non-steady-state component of the natural CO_2 fluxes, which we expect to drive most of the ocean flux

247   variability. The ability to constrain these sea-to-air CO_2 fluxes with observations has made large strides in the

248   last decade for at least three reasons. First was the expansion of the surface ocean partial pressure of CO_2 **[G]**

249   (pCO_2) measurement programs that began in the 1960s [93], but picked up momentum in the late 1980s and

250   1990s [94–96]. Second was the collation of the available surface ocean pCO_2 measurements by the Surface

251   Ocean CO_2 Atlas (SOCAT) effort into a quality controlled and openly accessible data product[97–99]. More than

252   30 million observations are in the SOCAT V2022 release, but these observations cover only a small fraction

253   of the ocean surface. For example, at any given month in the decade of the 2010s, only 3% of all 1°x 1° grid

254   points of the surface ocean have at least one observation. Therefore, the third notable advance was the

255   development of approaches to inter- and extrapolate these surface ocean pCO_2 observations to obtain space-

256   time continuous estimates of the sea-to-air CO_2 fluxes[100–102]. Six of these reconstructions have been

257   harmonized into a globally consistent product[103], called SeaFlux.

258   The long-term mean fluxes of this ensemble are characterized by strong outgassing of CO_2 in equatorial

259   regions, most prominently in the equatorial Pacific (Fig 2). There is a strong net uptake of CO_2 at latitudes

260   around 45° in both hemispheres. The overall pattern of the sources and sinks of CO_2 is primarily determined

261   by the exchange of natural CO_2, responding to heating and cooling, vertical transport and mixing, and

262   variations in biological productivity[9]. The uptake of anthropogenic CO_2 modifies these fluxes, most strongly

263   in the areas of large uptake of anthropogenic CO_2 such as the tropics and the high latitudes [104].

264   There is an almost doubling of the global net sea-to-air flux of CO_2 estimated by the SeaFlux ensemble from -

265   1.5 Pg C yr^{-1} in 1990 to -2.7 Pg C yr^{-1} in 2018 (Fig. 3a). A loss of natural CO_2 of 0.65 ± 0.30 Pg C yr^{-1} [105]

266   needs to be subtracted from the pCO_2 based estimates to compare these net fluxes with the global ocean

267   uptake estimates here (Table 1) and also those reported by the Global Carbon Project[1,51]. This loss is part of a

268   natural steady-state of the global carbon cycle, and results from the difference between the carbon input by

269   rivers and the carbon burial in marine sediments[105–108] (see also Box 1). Based on this information, the

270   combined fluxes of steady-state anthropogenic CO_2 and non-steady-state natural and anthropogenic CO_2 of -

271   2.1 ± 0.3 Pg C yr^{-1} in the 1990s, -2.3 ± 0.2 Pg C yr^{-1} in the 2000s, and -3.1 ± 0.2 Pg C yr^{-1} in the 2010s (Table 1)

272   (this flux is referred to as the ocean sink S_{OCEAN} in the Global Carbon Budget[1,51]).

273

274   *[H2] Interannual to decadal variability*

275   The overall trend from the 1990s to the present of about -0.4 Pg C yr^{-1} decade^{-1} is close to that estimated from

276   the steady-state model for anthropogenic CO_2 (orange dashed line in Fig 3a). The simulated fluxes from a

277   model run with constant circulation and constant biology (CESM-ETHZ)[25] show the same overall trend (red

278   dashed line), although with some more variations, largely reflecting changes in the growth rate of

279   atmospheric CO_2[33]. Thus, when analyzed over the last three decades, the surface ocean fluxes suggest an

280   ocean carbon sink that has increased at a rate commensurate with the steady-state prediction.

281   However, on interannual to decadal timescales, the ocean carbon sink diagnosed from the surface pCO_2

282   observations deviates substantially from the steady-state prediction (Fig 3a). The strongest deviations occur

283   on decadal timescales, with a weakening sink during the 1990s (a decadal trend of +0.3 Pg C yr^{-1} decade^{-1}

284   (1990-2001)), followed by a strong reinvigoration with a decadal trend of -0.7 Pg C yr^{-1} decade^{-1} (2002-

285   2018), nearly twice the rate from the steady state model. Integrated over the three decades, the ensemble

286   mean uptake is 6 ± 5 Pg C (11%) smaller than expected from the steady-state prediction, that is, this difference

287   suggests a non-steady-state or climate variability induced loss of natural and anthropogenic CO_2. The

288   estimates from the individual pCO_2-based reconstructions (shown in grey in Fig 3a) vary substantially around

289   the SeaFlux ensemble mean, but all agree on the strong decadal modulation of the ocean carbon sink around

290   the long-term trend.

291   All ocean basins contribute to the decadal variations of the ocean carbon sink, but the largest changes occur

292   in the Pacific Ocean and the Southern Ocean, which is defined here as the ocean south of 44°S [24,32,109,110] (Fig

293   3b). Both basins experienced a strong minimum in uptake around 2002 and a recovery thereafter, while the

294   Atlantic basin north of 44°S had a more gradual increase through time. The Pacific is the only basin that

295   exhibits a clear interannual variability signal on top of the trend and the decadal changes. In contrast, the

296   carbon sink of the Indian Ocean north of 44°S remained relatively constant.

297   Given that all these estimates rely on the same sparsely sampled ocean pCO_2 data, though, the potential for

298   systematic errors that transcends all interpolation methods cannot be excluded[111]. The reconstructions in the

299   Southern Hemisphere are particularly concerning, as model based analyses[111] suggest that the severe

300   undersampling could lead to an overestimating of the diagnosed decadal variability. In addition, the cool

301   surface ocean skin effect [112] and uncertainties associated with the functional dependence of the gas transfer

302   velocity on wind and other environmental factors[113] add to the overall uncertainty of the flux products.

303   Regardless, these variations—especially the weakening and strengthening periods—are seen in other,

304   independent estimates, including from forward models [25] and inverse models[114], although with generally

305   smaller magnitudes[23].

306

307

308   ***[H2] Patterns of variability***

309   More details about the spatio-temporal nature of the sea-to-air flux variations can be gleaned from the pCO_2

310   observation-based constraints that emerged in the 2010s. A Hovmoeller plot of the zonal integrals of the

311   anomalous air-sea fluxes (Fig 4a) shows that the largest variations occur in the regions of strong absolute

312   fluxes, that is, either in regions of strong uptake (temperate to high latitudes) or in the regions of strong

313   outgassing of CO_2 (tropics). On top of the year-to-year variations, which are most prominent in the tropical

314   latitudes, the long-term changes and the superimposed decadal variability clearly emerge from the data. They

315   indicate that the extratropics (between 30° and 60° latitude) were the most important latitudes contributing to

316   the rapid growth in the ocean carbon sink in the 2000s and 2010s, with the southern hemisphere dominating

317   due to its larger ocean surface area.

318   These fluxes are the sum of the anomalies of the anthropogenic and natural CO_2 flux components. To

319   separate them, the Ocean Inversion Project-based steady-state estimates for the uptake of anthropogenic CO_2

320   from the [72] for the year 1995 were scaled to the entire period using the β-based scaling approach used above.

321   The zonal integral of the anomalies of this steady-state component of the anthropogenic CO_2 flux indicates

322   that the regions of highest uptake in the Southern Ocean, the tropics and the mid latitudes of the northern

323   hemisphere imprint large trends on the fluxes in these regions. In contrast, other regions have only a small

324   trend in absolute terms (Fig 4b).

325   By removing this anthropogenic steady-state trend from the anomalous flux, the remaining anomalies reveal a

326   clearer picture of the non-steady-state components driven by climate variability (Fig 4c). The strong

327   interannual nature of the variations in the tropical belt emerges even more prominently. These anomalies are

328   correlated to the El Niño Southern Oscillation (ENSO) [G], as indicated by the negative correlation of the

329   zonal anomalies in the tropical belt with the multivariate ENSO index[115] (R = -0.79, p<0.05). However, the

330   anomalous uptake during El Niños was strong in the 1990s and weakened substantially after the turn of the

331   millennium. At the same time, the anomalous outgassing during La Niña conditions strengthened over time.

332   These ENSO related trends yield a distinct decadal signal in the tropics as well, characterized by an

333   anomalous uptake during the 1990s, neutral conditions during the first decade of the new millennium, and

334   anomalous outgassing in the 2010s.

335   The decadal nature of the Southern Ocean sink variability is also more discernible in these non-steady-state

336   fluxes (Fig 4c). Over the course of the 1990s, there was a rapid change from an anomalous uptake to an

337   anomalous outgassing peaking around 2002. This was followed by a prolonged period of anomalous

338   outgassing until about 2008 and a recovery to normal conditions around 2010. Thus, the strong trend in the

339   Southern Ocean toward increasing uptake in the last two decades is largely the result of the strong trend

340   imparted by the steady-state uptake of anthropogenic CO_2, reflecting the major role of the this region in

341   taking up anthropogenic CO_2 from the atmosphere (Fig 4b) [72,116].

342   The trend from an anomalous sink to an anomalous source during the 1990s followed by a strengthening

343   period after 2000 is also evident across most latitudes of the northern hemisphere (Fig 4c). This co-

344   occurrence suggests that apart from the tropics, the decadal mode of sea-to-air CO_2 flux variability has a

345   global component, even after accounting for the steady-state trend in the uptake flux of anthropogenic CO_2.

346   In summary, the pCO_2 observation-based constraints on the sea-to-air CO_2 fluxes that have emerged in the

347   last decade have reshaped our understanding of the variability of the ocean carbon sink (Figure 5). In

348   particular, the surface flux products have suggested the presence of an important decadal mode of variability

349   in the extra-tropics, and particularly in the Southern Ocean (Figure 5). This observation contrasts with the

350   results of ocean biogeochemical models, whose variability tend to be, on average, smaller, and also which

351   tend to have most of the variability focused in the tropics [25,30,117]. Nevertheless, the models also simulate

352   decadal variability in the extratropics [23,25,28,29,118]), adding further evidence that the decadal variability

353   diagnosed from the observations is a robust feature.

354

355   *[H2] Mechanisms of variability*

356

357   Variations in the ocean carbon sink can either be caused by processes that are internal to the climate system

358   or can be externally forced. Internal forcing is associated with variations in weather and climate

359   [24,27,28,32,109,114,119] including changes associated with anthropogenic climate change[120]. Externally forced

360   variations are caused by changes outside the climate system, such as those induced by the volcanic eruption

361   of Mount Pinatubo in 1991[33]. Such an eruption can impact the ocean carbon sink through changes in both

362   Earth surface temperature and atmospheric CO_2 growth rate.

363   Interannual variations in the ocean carbon sink are driven by internal processes, as they are associated with

364   the ENSO-related year-to-year variations in the sea-to-air fluxes in the tropical Pacific[30,121–123]. During El

365   Niño conditions, reduced upwelling and thermocline deepening in the Eastern Tropical Pacific strongly

366   decrease the vertical supply of DIC to the surface. This process causes a collapse of the high pCO_2 levels that

367   drive CO_2 out of the ocean, even though sea-surface temperatures are warmer than normal. Reduced

368   windspeeds during El Niño conditions tend to further reduce the outgassing and thus enhance the effect of the

369   reduced supersaturation[123]. The resulting sea-to-air flux anomalies are sizable and impact the regional

370   atmospheric CO_2 concentration[124]. The flux variations are most likely almost entirely driven by changes in

371   the natural CO_2, in particular its non-steady-state component (Fig 4c).

372   Mechanisms driving the decadal variations in the ocean carbon sink are less understood. One argument is that

373   at least part of the variations are externally forced[33], as the eruption of Mt Pinatubo in 1991 caused both a

374   reduced growth rate of atmospheric CO_2 during much of the 1990s [125–127] and a global cooling trend in the

375   surface temperature. The low growth rate reduces the ocean carbon sink directly by modifying the air-sea

376   pCO_2 gradient. This effect would be enhanced by the upper ocean cooling and the associated enhanced ocean

377   mixing caused by the global cooling [128,129]. According to this argument, these two processes would have

378   reduced the oceanic uptake during the 1990, while the resumption of higher atmospheric CO_2 growth rates

379   thereafter would have caused the ocean uptake to rebound [33].

380   An alternative line of arguments is that these decadal changes are the result of processes that are internal to

381   the climate system. For example, a poleward contraction and intensification of the westerly wind belt around

382   Antarctica might have caused the weakening trend of the Southern Ocean carbon sink during the 1990s[28],

383   driven primarily by a trend toward a positive phase of the Southern Annular Mode [G] (SAM)[130]. The

384   stronger winds led to more upwelling of CO_2 and nutrient rich deep water, increasing CO_2 outgassing (albeit

385   partly balanced by stronger biological production) [28,118,131,132]. Then, a shift to a zonally more undulating

386   windfield coupled with changes in sea-surface temperature caused the reinvigoration of the Southern Ocean

387   carbon sink thereafter[32]. At least a part of these wind changes, and especially those of the 1990s, have been

388   attributed to anthropogenic warming and ozone loss forcing the positive trend in the SAM[133]. Simulations

389   suggest that the majority of the response of the CO_2 fluxes is driven by changes in the natural CO_2

390   component, with the fluxes of anthropogenic CO_2 modulating the response, often in opposite directions, thus

391   moderating the effect [24,28,114,132].

392   In contrast to the Southern Ocean, the potential mechanisms causing the reconstructed increases in the carbon

393   sink in the northern hemisphere after 2000 are not well investigated. They most likely mechanisms involve

394   changes in winds, changes in temperature affecting the solubility, changes in buoyancy forcing affecting

395   winter mixed layers[134], and large-scale gyre changes[27]. The latter are potentially associated with changes in

396   the northern annular mode (NAM) or associated northern hemisphere modes of variability [109].

397   The relative roles of internal versus external forcing driving the reconstructed decadal variations still need to

398   be firmly established. Simulations with a changing atmospheric CO_2 growth rate, but no changes in climate,

399   suggest that the effect is visible, albeit much smaller than the observed changes (the dashed red versus orange

400   line in Fig 3a). The effect of the cooling and warming pattern associated with Mt. Pinatubo is more difficult

401   to quantify independently, but simulations with comprehensive ocean biogeochemical models [G] [128,135]

402   suggest an effect ≤ 0.2 Pg C yr^{-1} during peak cooling, and rapidly decreasing thereafter. However, the ocean

403   carbon sinks changing globally relatively synchronously supports that there was an external forcing

404   mechanism (Fig 4). Overall, external forcing (such as by volcanos) and internal changes (as by weather and

405   climate variability) are not mutually exclusive processes, and both likely play a role in driving ocean carbon

406   sink variability.

407

408   *[H2] Merging observational constraints*

409   Bringing together the ocean interior constraints on the evolution of the ocean sink with those provided by the

410   surface ocean measurements can help to better understand the mechanisms driving trends and variability

411   (Table 1). The estimates of the ocean interior accumulation of anthropogenic CO_2 suggest an ocean that

412   globally has operated near steady-state. The extrapolation with β-scaling suggests a cumulative uptake of

413   about 83 Pg C between 1990 and 2018. The reconstructions of the surface fluxes, which include both natural

414   and anthropogenic CO_2 components, suggest 6±5 Pg C less uptake over the same period (Table 1, Fig 3a).

415   This reduction is mostly attributed to a non-steady-state loss of natural CO_2, as the simulation with the

416   observed variations in atmospheric CO_2 suggested a small change in the total uptake of anthropogenic CO_2

417   (red versus orange dashed lines in Fig 3). This loss needs to be taken into consideration when constructing

418   global carbon budgets with ocean interior inventory changes. Indeed, a potential loss of 5±3 Pg C was

419   considered in the global assessment of the accumulation of anthropogenic CO_2 for the period 1994 through

420   2007[4]. In addition to circulation driven decadal variability, a part of this loss could be caused by ocean

421   warming, as a warming induced loss of 5±1 Pg C between 1990 and 2000[136] has been suggested (Table 1).

422   These losses and the corresponding budget adjustments are currently very tentative, and urgently require

423   verifications through direct observations of changes in the oceanic DIC pool, for example.

424   While ocean interior and surface ocean constraints are becoming more consistent, new discrepancies have

425   arisen. Most prominent is a growing difference between the ocean sink estimates based on surface ocean

426   pCO_2 observations and those based on ocean biogeochemical models. These estimates agree well during the

427   first decade of the millennium, but diverge thereafter, with the observation-based estimates indicating a much

428   larger growth in the uptake than the models[1,25] (Table 1). This difference is also evident in these models

429   yielding a relatively low sensitivity β of 1.11±0.18 Pg C / ppm CO_2 for the period 1990 through 2018 (Fig 1a,

430   Supplementary Table 1). One reason is that the presently used models tend to underestimate the uptake of

431   anthropogenic CO_2, as evidenced by direct comparison with the uptake estimates stemming from the

432   accumulation of anthropogenic CO_2 (Fig 1b,c)[1]. A model-based emergent constraint approach on a different,

433   but related set of models suggests an underestimation of about 10% [137]. Adjusting the models for this bias

434   halves the mismatch between models and observations-based estimates for the period after 2010, but opens

435   larger discrepancies in the earlier decades. The uncertainties in the observation-based flux products stemming

436   from the sparse observations, and issues at the tails of the observational-based time-series[112] might contribute

437   to these discrepancies.

438

439   **[H1] SUMMARY AND FUTURE PERSPECTIVES**

440   The strength of the ocean carbon sink has tripled from the 1960s until the present. Thus, the ocean has

441   maintained its key role as a sink for the CO_2 emitted into the atmosphere as a consequence of human

442   activities, removing about 25±2% of the total emissions over six decades. The strengthening of the ocean sink

443   has been largely driven by the increasing uptake of anthropogenic CO_2 in response to the rise in atmospheric

444   CO_2, leading to a strong proportionality between the two. In contrast, the contribution from changes in the

445   natural carbon cycle has been small so far, consistent with the assumption that the ocean circulation and

446   biological pump was overall in steady-state. However, new insights and observations in the past decade

447   challenge this assumption, especially on shorter timescales, suggesting an ocean that is more variable than

448   previously recognized. New evidence also suggests over the past three decades a loss of natural CO_2 to the

449   atmosphere due to ocean warming and changes in ocean circulation. If confirmed, such a loss suggests an

450   ocean carbon sink that is rather vulnerable to climate change.

451   An ocean sink that is more vulnerable to climate change than currently assumed in coupled carbon-climate

452   models[52] would imply that the ocean will take up less CO_2 from the atmosphere in the future than anticipated.

453   This would leave a larger fraction of the emissions in the atmosphere, causing additional global warming and

454   climate change. In other words, the ocean carbon-climate feedback could be more positive than suggested by

455   current coupled carbon-climate models. Moreover, the finding of the ocean sink potentially being more

456   sensitive to changes in atmospheric CO_2 growth rates than previously recognized, implies a stronger than

457   anticipated decline of the ocean carbon sink in ambitious mitigation scenarios [34,138].

458   The implications are large and far-reaching. Any reduction in ocean carbon uptake compared to current

459   assumptions would require even stronger investments into decarbonization strategies, making the

460   achievement of specific global warming targets harder. It also reduces the efficacy of the negative emission

461   approaches that aim to curb climate change by removing CO_2 from the atmosphere using land-based[139,140] or

462   ocean-based[141] approaches.

463   To better constrain and predict the ocean carbon sink, there are three important challenges to address: the

464   robustness of the reconstructed changes and variations; the processes driving these changes and variations;

465   and predictions of the future ocean uptake, in particular the response of the ocean carbon sink to future

466   climate change, the reduction in anthropogenic CO_2 emissions, and the potential deployment of carbon

467   dioxide removal technologies. Addressing these challenges is important both scientifically and for policy. For

468   example, during the upcoming Global Stocktake undertaken within the U.N. Framework Convention on

469   Climate Change (UNFCCC), reliable estimates of the ocean carbon sink will be a crucial element to close the

470   global carbon budget. In addition, the study of ocean-based carbon dioxide removal approaches, such as

471   ocean alkalinization, nutrient fertilization, seaweed growth, and artificial upwelling, have gained

472   momentum[141], requiring a thorough assessment of their effectiveness and consequences.

473   In our view, the following measures must be taken to answer these challenges (see also Ref[142]). The existing

474   observation networks need to be improved, expanded, and put on a much better long-term funding level. The

475   limited sampling of the ocean carbon system is currently the largest source of uncertainty in assessing the

476   variability of the ocean carbon sink. The current sampling is sufficient to capture the long-term time mean

477   sink, and the year-to-year variations in the tropical Pacific and a few other regions, especially in the northern

478   hemisphere where the sampling is relatively dense. In contrast, sampling is critical in many other key regions,

479   such as the Southern Ocean, the South Pacific and the Indian Ocean. Higher resolution observations in time

480   and space will also help to better understand the processes leading to these variations, including those that

481   lead to extremes in ocean acidification and/or deoxygenation[143]. Ocean observing system simulation

482   experiments can help to determine where and when the observing density has to be increased, and to suggest

483   optimal combinations of different observing platforms[144,145].

484   To support observation, new technologies—especially those that enhance the ability to observe ocean carbon

485   in an autonomous manner—need to be developed, improved, and strategically deployed. Improvement of

486   analytical techniques, sensor technology and calibration methods for ocean carbon measurements is urgently

487   required for the provision of accurate, well-calibrated ocean carbon measurements, while improving the ease

488   and efficiency of data collection, thus increasing the scope for autonomous data collection and reducing the

489   cost of these measurements, such as the Biogeochemical Argo program[146–148].

490   To build on expanded and improved sampling, the existing ocean carbon synthesis projects (GLODAP and

491   SOCAT) and the downstream efforts such as the Global Carbon Budget (GCB) and SeaFlux need to be

492   strengthened and expanded. A more rapid update of the analyses, such as on a semi-annual basis providing

493   closer to real-time analyses of the global carbon budget, could be useful to better linking the ocean to the

494   Global Stocktake activities. Similarly, models and observations need to be better integrated, especially

495   through data assimilation and interpolation approaches[149–151]. As part of this effort, these models should be

496   pushed to resolve smaller spatial and temporal scales, better capturing the small-scale variability that is

497   inherent in the data that is collected and assimilated by these models. If these models can resolve both the

498   large scales that are representative of global budgets, and the small scales that are representative of the

499   observations, they will be able to more accurately reflect our state of knowledge and its uncertainty.

500

501   Moving beyond carbon measurements and budgets, focused process studies need to be developed to better

502   understand critical processes. The need to improve knowledge of the sensitivity of ocean biology to changes

503   in temperature, ocean acidification and other parameters is pressing. In addition researchers need a better

504   understanding of the aquatic continuum[105]—the aquatic network that connects the land aquatic systems to the

505   ocean, delivering inorganic and organic matter to the ocean, whose fate is critical to determine the outgassing

506   of river-derived CO_2. Although a value of 0.65 Pg C yr^{-1} for the degassing of terrestrially-derived CO_2 was

507   used here and in the Global Carbon Budget [1], individual estimates range between 0.2 Pg C yr^{-1} [152] and 1.2 Pg

508   C yr^{-1} [153], reflecting the large uncertainty of this estimate. An especially under-investigated area is the fate of

509   the river-derived carbon in the ocean, and in particular, the determination of how much carbon is buried in

510   sediments close to the river mouths, how much enters the open ocean and how fast this carbon is

511   remineralized back to CO_2 [152].

512   The role of the ocean in taking up additional CO_2 in response to the deployment of carbon dioxide removal

513   technologies needs to be critically evaluated. There must be a particular focus on the efficacy of these

514   measures and their potential for negative (unintended) consequences[154]. Historically, the ocean sink for

515   carbon has been considered as very robust to changes, and largely tracking the increase in atmospheric CO_2.

516   It is time to change this perspective and to recognize that the ocean carbon cycle might be more sensitive to

517   change than previously recognized. The size of this sink, its unknown response to a reduction in

518   anthropogenic CO_2 emissions and its relevance for past and future climates are large enough to warrant

519   renewed efforts to observe it, to study it, and to understand it.

520

521

References

Top references

(1) Friedlingstein et al. (2022)
Most recent version of the Global Carbon Budget, an international effort led by the Global Carbon
Project to synthesize all components of the global carbon cycle.

(2) Sabine et al. (2004)
First observation-based global inventory of anthropogenic CO_2 providing a key constraint for the
global anthropogenic CO_2 budget.

(3) Khatiwala et al. (2009)
Reconstruction of the entire history of the oceanic uptake of anthropogenic CO_2.

(4) Gruber et al. (2019)
Inventory of anthropogenic CO_2 that provided a second time-point describing the accumulation of
anthropogenic CO2 in the ocean based on ocean interior observations.

(25) Hauck et al. (2020)
Description and assessment of the ocean biogeochemical models currently used to determine the
oceanic uptake of CO_2 in the context of the Global Carbon Budget.

(30) Le Quéré et al., (2007)
First study to point out that the Southern Ocean carbon sink weakened substantially during the 1990s.

(32) Landschützer et al. (2016)
Assessment of the decadal variability of the ocean carbon sink that reveals it is driven by the
extratropical latitudes in both hemispheres.

(72) Mikaloff-Fletcher et al. (2006)
Ocean inversion-based study describing the regional distribution of the air-sea fluxes of anthropogenic
CO_2 and its oceanic transport.

560   *References by number:*
561
562   1.   Friedlingstein, P. *et al.* Global Carbon Budget 2021. *Earth Syst. Sci. Data* **14**, 1917–2005 (2022).
563   2.   Sabine, C. L. *et al.* The Oceanic Sink for Anthropogenic CO 2. *Science (80-.).* **305**, 367–371 (2004).
564   3.   Khatiwala, S., Primeau, F. & Hall, T. Reconstruction of the history of anthropogenic CO2
565   concentrations in the ocean. *Nature* **462**, 346–349 (2009).
566   4.   Gruber, N. *et al.* The oceanic sink for anthropogenic CO 2 from 1994 to 2007. *Science (80-.).* **363**,
567   1193–1199 (2019).
568   5.   Revelle, R. Introduction: The scientific history of carbon dioxide. in *The Global Carbon Cycle and*
569   *atmospheric CO_2: Natural Variations Archean to Present* (eds. Sundquist, E. T. & Broecker, W. S.)
570   1–4 (AGU, 1985).
571   6.   Heimann, M. A review of the contemporary global carbon cycle and as seen a century ago by
572   Arrhenius and Hogbom. *Ambio* **26**, 17–24 (1997).
573   7.   Arrhenius, S. *Lehrbuch der kosmischen Physik*. **2**, (Hirzel, 1903).
574   8.   Archer, D., Kheshgi, H. & Maier-Reimer, E. Multiple timescales for neutralization of fossil fuel CO 2.
575   *Geophys. Res. Lett.* **24**, 405–408 (1997).
576   9.   Sarmiento, J. L. & Gruber, N. *Ocean Biogeochemical Dynamics*. (Princeton University Press, 2006).
577   10.   Callendar, G. S. The artificial production of carbon dioxide and its influence on climate. *Q. J. R.*
578   *Meteor. Soc.* **64**, 223–240 (1938).
579   11.   Revelle, R. & Suess, H. E. Carbon Dioxide Exchange between Atmosphere and Ocean and the
580   question of an increase of atmospheric {CO}_2 during the past decades. *Tellus* **9**, 18–27 (1957).
581   12.   Revelle, R., Broecker, W. S., Craig, H., Keeling, C. D. & Smagorinsky, J. *Atmospheric Carbon*
582   *Dioxide*. (1965).
583   13.   Charney, J. G. *et al. Carbon Dioxide and Climate: A scientific assessment*. (1979).
584   14.   Keeling, C. D. The concentration and isotopic abundances of carbon dioxide in the atmosphere. *Tellus*
585   **12**, 200–203 (1960).
586   15.   W.R.Wallace, D. Chapter 6.3 Storage and transport of excess CO2 in the oceans:The JGOFS/WOCE
587   global CO2 survey. in *Ocean circulation and climate* (eds. Siedler, G., Church, J. & Gould, J.) 489–L
588   (Academic Press, 2001). doi:10.1016/S0074-6142(01)80136-4
589   16.   Keppler, L., Landschützer, P., Gruber, N., Lauvset, S. K. & Stemmler, I. Seasonal Carbon Dynamics
590   in the Near-Global Ocean. *Global Biogeochem. Cycles* **34**, (2020).
591   17.   Canadell, P. G. *et al.* Global Carbon and other Biogeochemical Cycles and Feedbacks. in *Climate*
592   *Change 2021: The Physical Science Basis. Contribution of Working Group I to the Sixth Assessment*
593   *Report of the Intergovernmental Panel on Climate Change* 673–816 (2021).
594   doi:10.1017/9781009157896.007
595   18.   Oeschger, H., Siegenthaler, U., Schotterer, U. & Gugelmann, A. A box diffusion model to study the
596   carbon dioxide exchange in nature. *Tellus* **27**, 168–192 (1975).
597   19.   Brewer, P. G. Direct observation of the oceanic {CO}_2 increase. *Geophys. Res. Lett.* **5**, 997–1000
598   (1978).
599   20.   Chen, C.-T. A. & Millero, F. J. Gradual increase of oceanic CO2. *Nature* **277**, 205–206 (1979).
600   21.   Sabine, C. L. & Tanhua, T. Estimation of Anthropogenic CO 2 Inventories in the Ocean. *Ann. Rev.*
601   *Mar. Sci.* **2**, 175–198 (2010).
602   22.   Olsen, A. *et al.* The Global Ocean Data Analysis Project version 2 (GLODAPv2) – an internally
603   consistent data product for the world ocean. *Earth Syst. Sci. Data* **8**, 297–323 (2016).
604   23.   DeVries, T. *et al.* Decadal trends in the ocean carbon sink. *Proc. Natl. Acad. Sci.* **116**, 201900371
605   (2019).
606   24.   Gruber, N., Landschützer, P. & Lovenduski, N. S. The Variable Southern Ocean Carbon Sink. *Ann.*
607   *Rev. Mar. Sci.* **11**, 159–186 (2019).
608   25.   Hauck, J. *et al.* Consistency and Challenges in the Ocean Carbon Sink Estimate for the Global Carbon
609   Budget. *Front. Mar. Sci.* **7**, 1–33 (2020).
610   26.   Landschützer, P., Gruber, N., Bakker, D. C. E. & Schuster, U. Recent variability of the global ocean

611   carbon sink. *Global Biogeochem. Cycles* **28**, 927–949 (2014).

612   27.   Landschützer, P., Gruber, N. & Bakker, D. C. E. Decadal variations and trends of the global ocean
613   carbon sink. *Global Biogeochem. Cycles* **30**, 1396–1417 (2016).

614   28.   Le Quere, C. *et al.* Saturation of the Southern Ocean CO2 Sink Due to Recent Climate Change.
615   *Science (80-.).* **316**, 1735–1738 (2007).

616   29.   Lovenduski, N. S., Gruber, N., Doney, S. C. & Lima, I. D. Enhanced CO 2 outgassing in the Southern
617   Ocean from a positive phase of the Southern Annular Mode. *Global Biogeochem. Cycles* **21**, n/a-n/a
618   (2007).

619   30.   Le Quéré, C., Orr, J. C., Monfray, P., Aumont, O. & Madec, G. Interannual variability of the oceanic
620   sink of CO 2 from 1979 through 1997. *Global Biogeochem. Cycles* **14**, 1247–1265 (2000).

621   31.   Fay, A. R. & McKinley, G. A. Global trends in surface ocean p CO 2 from in situ data. *Global*
622   *Biogeochem. Cycles* **27**, 541–557 (2013).

623   32.   Landschützer, P. *et al.* The reinvigoration of the Southern Ocean carbon sink. *Science (80-.).* **349**,
624   1221–1224 (2015).

625   33.   McKinley, G. A., Fay, A. R., Eddebbar, Y. A., Gloege, L. & Lovenduski, N. S. External Forcing
626   Explains Recent Decadal Variability of the Ocean Carbon Sink. *AGU Adv.* **1**, 1–10 (2020).

627   34.   Rogelj, J. *et al.* Mitigation Pathways Compatible with 1.5°C of Sustainable Development. in *Global*
628   *warming of 1.5°C. An IPCC Special Report [...]* 93–174 (2018).

629   35.   Cheng, L. *et al.* Another Record: Ocean Warming Continues through 2021 despite La Niña
630   Conditions. *Adv. Atmos. Sci.* (2022). doi:10.1007/s00376-022-1461-3

631   36.   Abram, N. *et al.* Chapter 1: Framing and Context of the Report. in *Special Report on the Ocean and*
632   *Cryosphere (SROCC)* (eds. Pörtner, H.-O. et al.) (2019).

633   37.   Bindoff, N. L. *et al.* Chapter 5: Changing Ocean, Marine Ecosystems, and Dependent Communities.
634   in *Special Report on the Ocean and Cryosphere (SROCC)* (eds. Pörtner, H.-O. et al.) (2019).

635   38.   Sarmiento, J. L., Orr, J. C. & Siegenthaler, U. A perturbation Simulation of CO2 uptake in an Ocean
636   General Circulation Model. *J. Geophys. Res.* **97**, 3621–3645 (1992).

637   39.   Matsumoto, K. Radiocarbon-based circulation age of the world oceans. *J. Geophys. Res.* **112**, 1–7
638   (2007).

639   40.   Holzer, M. & Primeau, F. W. The path-density distribution of oceanic surface-to-surface transport. *J.*
640   *Geophys. Res. Ocean.* **113**, 1–22 (2008).

641   41.   Dong, Y. *et al.* Update on the Temperature Corrections of Global Air-Sea CO 2 Flux Estimates.
642   *Global Biogeochem. Cycles* **26**, 21–35 (2022).

643   42.   Matsumoto, K. & Gruber, N. How accurate is the estimation of anthropogenic carbon in the ocean?
644   An evaluation of the Δ C * method. *Global Biogeochem. Cycles* **19**, (2005).

645   43.   Bates, N. *et al.* A Time-Series View of Changing Ocean Chemistry Due to Ocean Uptake of
646   Anthropogenic CO2 and Ocean Acidification. *Oceanography* **27**, 126–141 (2014).

647   44.   Gregor, L. & Gruber, N. OceanSODA-ETHZ: a global gridded data set of the surface ocean carbonate
648   system for seasonal to decadal studies of ocean acidification. *Earth Syst. Sci. Data* **13**, 777–808
649   (2021).

650   45.   Broecker, W. S., Takahashi, T., Simpson, H. J. & Peng, T. H. Fate of fossil fuel carbon dioxide and
651   the global carbon budget. *Science (80-.).* **206**, 409–418 (1979).

652   46.   Egleston, E. S., Sabine, C. L. & Morel, F. M. M. Revelle revisited: Buffer factors that quantify the
653   response of ocean chemistry to changes in DIC and alkalinity. *Global Biogeochem. Cycles* **24**, 1–9
654   (2010).

655   47.   Jiang, L. Q., Carter, B. R., Feely, R. A., Lauvset, S. K. & Olsen, A. Surface ocean pH and buffer
656   capacity: past, present and future. *Sci. Rep.* **9**, 18624 (2019).

657   48.   Sarmiento, J. L., LeQuéré, C. & Pacala, S. W. Limiting future atmospheric carbon dioxide. *Glob.*
658   *Biogeochem. Cycles* **9**, 121–137 (1995).

659   49.   Joos, F. *et al.* An efficient and accurate representation of complex oceanic and biospheric models of
660   anthropogenic carbon uptake. *Tellus* **48B**, 397–417 (1996).

661   50.   Keeling, C. D. The Suess Effect: 13-Carbon and 14-Carbon Interactions. in *Environment International*

662   **2**, 229–300 (Pergamon, 1979).

663   51.   Friedlingstein, P. *et al.* Global Carbon Budget 2020. *Earth Syst. Sci. Data* **12**, 3269–3340 (2020).

664   52.   Arora, V. K. *et al.* Carbon–concentration and carbon–climate feedbacks in CMIP6 models and their
665   comparison to CMIP5 models. *Biogeosciences* **17**, 4173–4222 (2020).

666   53.   Friedlingstein, P. *et al.* Climate-carbon cycle feedback analysis: results from the {C4MIP} model
667   intercomparison. *J. Clim.* **19**, 3337–3353 (2006).

668   54.   Meinshausen, M. *et al.* Realization of Paris Agreement pledges may limit warming just below 2 °C.
669   *Nature* **604**, 304–309 (2022).

670   55.   Joos, F. *et al.* Carbon dioxide and climate impulse response functions for the computation of
671   greenhouse gas metrics: A multi-model analysis. *Atmos. Chem. Phys.* **13**, 2793–2825 (2013).

672   56.   Waugh, D. W., Hall, T. M., Mcneil, B. I., Key, R. & Matear, R. J. Anthropogenic CO 2 in the oceans
673   estimated using transit time distributions. *Tellus B Chem. Phys. Meteorol.* **58**, 376–389 (2006).

674   57.   Tanhua, T. *et al.* Ventilation of the Arctic Ocean: Mean ages and inventories of anthropogenic CO2
675   and CFC-11. *J. Geophys. Res.* **114**, 1–11 (2009).

676   58.   Raimondi, L., Tanhua, T., Azetsu-Scott, K., Yashayaev, I. & Wallace, D. W. R. A 30 -Year Time
677   Series of Transient Tracer-Based Estimates of Anthropogenic Carbon in the Central Labrador Sea. *J.*
678   *Geophys. Res. Ocean.* **126**, 1–19 (2021).

679   59.   Ridge, S. M. & McKinley, G. A. Ocean carbon uptake under aggressive emission mitigation.
680   *Biogeosciences* **18**, 2711–2725 (2021).

681   60.   Archer, D., Kheshgi, H. & Maier-Reimer, E. Dynamics of fossil fuel {CO}_2 neutralization by marine
682   {CaCO}_3. *Glob. Biogeochem. Cycles* **12**, 259–276 (1998).

683   61.   Bacastow, R. B. & Keeling, C. D. Models to predict future atmospheric CO2 concentrations. in
684   *Workshop on the Global Effects of Carbon Dioxide from Fossil Fuels* (eds. Elliott, W. P. & Machta,
685   L.) 72–90 (United States Department of Energy, 1979).

686   62.   Siegenthaler, U. & Oeschger, H. Predicting future atmospheric carbon dioxide levels. *Science* **199**,
687   388–95 (1978).

688   63.   Wallace, D. W. R. *Monitoring Global Ocean Carbon Inventories*. (1995).

689   64.   Gruber, N., Sarmiento, J. L. & Stocker, T. F. An improved method for detecting anthropogenic CO 2
690   in the oceans. *Global Biogeochem. Cycles* **10**, 809–837 (1996).

691   65.   Gruber, N. Anthropogenic CO 2 in the Atlantic Ocean. *Global Biogeochem. Cycles* **12**, 165–191
692   (1998).

693   66.   Dickson, A. G., Goyet, C. & DOE. *Handbook of methods for the analysis of the various parameters of*
694   *the carbon dioxide system in sea water; version 2*. (1994).

695   67.   Dickson, A. G., Afghan, J. D. & Anderson, G. C. Reference materials for oceanic {CO}_2 analysis: a
696   method for the certification of total alkalinity. *Mar. Chem.* **80**, 185–197 (2003).

697   68.   Dickson, A. G. Standards for ocean measurements. *Oceanography* **23**, 34–47 (2010).

698   69.   Key, R. M. *et al.* A global ocean carbon climatology: Results from Global Data Analysis Project
699   (GLODAP). *Global Biogeochem. Cycles* **18**, n/a-n/a (2004).

700   70.   DeVries, T. The oceanic anthropogenic CO 2 sink: Storage, air-sea fluxes, and transports over the
701   industrial era. *Global Biogeochem. Cycles* **28**, 631–647 (2014).

702   71.   Orr, J. C. *et al.* Estimates of anthropogenic carbon uptake from four three-dimensional global ocean
703   models. *Global Biogeochem. Cycles* (2001).

704   72.   Mikaloff Fletcher, S. E. *et al.* Inverse estimates of anthropogenic CO2 uptake, transport, and storage
705   by the ocean. *Global Biogeochem. Cycles* **20**, 1–16 (2006).

706   73.   Davila, X. *et al.* How Is the Ocean Anthropogenic Carbon Reservoir Filled? *Global Biogeochem.*
707   *Cycles* **36**, 1–16 (2022).

708   74.   Groeskamp, S., Lenton, A., Matear, R., Sloyan, B. M. & Langlais, C. Anthropogenic carbon in the
709   ocean-Surface to interior connections. *Global Biogeochem. Cycles* **30**, 1682–1698 (2016).

710   75.   Keeling, R. F. & Shertz, S. R. Seasonal and interannual variations in atmospheric oxygen and
711   implications for the global carbon cycle. *Nature* **358**, 723–727 (1992).

712   76.   Quay, P. D., Tilbrook, B. & Wong, C. S. Oceanic Uptake of Fossil Fuel CO 2 : Carbon-13 Evidence.

713   *Science (80-.).* **256**, 74–79 (1992).

714 77. Heimann, M. & Maier-Reimer, E. On the relations between the oceanic uptake of CO2 and its carbon
715   isotopes. *Global Biogeochem. Cycles* **10**, 89–110 (1996).

716 78. Gruber, N. & Keeling, C. D. An improved estimate of the isotopic air-sea disequilibrium of CO 2 :
717   Implications for the oceanic uptake of anthropogenic CO 2. *Geophys. Res. Lett.* **28**, 555–558 (2001).

718 79. Khatiwala, S. *et al.* Global ocean storage of anthropogenic carbon. *Biogeosciences* **10**, 2169–2191
719   (2013).

720 80. Friedrich, T. *et al.* Detecting regional anthropogenic trends in ocean acidification against natural
721   variability. *Nature* **2**, 167–171 (2012).

722 81. Munro, D. R. *et al.* Recent evidence for a strengthening CO 2 sink in the Southern Ocean from
723   carbonate system measurements in the Drake Passage (2002-2015). *Geophys. Res. Lett.* **42**, 7623–
724   7630 (2015).

725 82. Talley, L. D. *et al.* Changes in Ocean Heat, Carbon Content, and Ventilation: A Review of the First
726   Decade of GO-SHIP Global Repeat Hydrography. *Ann. Rev. Mar. Sci.* **8**, 185–215 (2016).

727 83. Wanninkhof, R. *et al.* Detecting anthropogenic CO2 changes in the interior Atlantic Ocean between
728   1989 and 2005. *J. Geophys. Res.* **115**, C11028 (2010).

729 84. Friis, K., Körtzinger, A., Pätsch, J. & Wallace, D. W. R. On the temporal increase of anthropogenic
730   CO2 in the subpolar North Atlantic. *Deep. Res. Part I* **52**, 681–698 (2005).

731 85. Goodkin, N. F., Levine, N. M., Doney, S. C. & Wanninkhof, R. Impacts of temporal CO 2 and climate
732   trends on the detection of ocean anthropogenic CO 2 accumulation. *Global Biogeochem. Cycles* **25**, 1–
733   11 (2011).

734 86. Levine, N. M., Doney, S. C., Wanninkhof, R., Lindsay, K. & Fung, I. Y. Impact of ocean carbon
735   system variability on the detection of temporal increases in anthropogenic CO 2. *J. Geophys. Res.* **113**,
736   C03019 (2008).

737 87. Carter, B. R. *et al.* Two decades of Pacific anthropogenic carbon storage and ocean acidification along
738   Global Ocean Ship-based Hydrographic Investigations Program sections P16 and P02. *Global*
739   *Biogeochem. Cycles* **31**, 306–327 (2017).

740 88. Carter, B. R. *et al.* Pacific Anthropogenic Carbon Between 1991 and 2017. *Global Biogeochem.*
741   *Cycles* 2018GB006154 (2019). doi:10.1029/2018GB006154

742 89. Woosley, R. J., Millero, F. J. & Wanninkhof, R. Rapid anthropogenic changes in CO 2 and pH in the
743   Atlantic Ocean: 2003-2014. *Global Biogeochem. Cycles* **30**, 70–90 (2016).

744 90. Clement, D. & Gruber, N. The eMLR(C*) Method to Determine Decadal Changes in the Global
745   Ocean Storage of Anthropogenic CO 2. *Global Biogeochem. Cycles* **32**, 654–679 (2018).

746 91. Tanhua, T., Körtzinger, A., Friis, K., Waugh, D. W. & Wallace, D. W. R. An estimate of
747   anthropogenic CO2 inventory from decadal changes in oceanic carbon content. *Proc. Natl. Acad. Sci.*
748   **104**, 3037–3042 (2007).

749 92. Pérez, F. F. *et al.* Atlantic Ocean CO2 uptake reduced by weakening of the meridional overturning
750   circulation. *Nat. Geosci.* **6**, 146–152 (2013).

751 93. Keeling, C. D. Carbon Dioxide in Surface Ocean Waters: 4. Global Distribution. *J. Geophys. Res.* **73**,
752   4543–4553 (1968).

753 94. Tans, P. P., Fung, I. Y. & Takahashi, T. Observational Contrains on the Global Atmospheric Co 2
754   Budget. *Science (80-.).* **247**, 1431–1438 (1990).

755 95. Takahashi, T. *et al.* Global air-sea flux of CO 2 : An estimate based on measurements of sea–air pCO
756   2 difference. *Proc. Natl. Acad. Sci.* **94**, 8292–8299 (1997).

757 96. Takahashi, T. *et al.* Deep-Sea Research II Climatological mean and decadal change in surface ocean
758   pCO 2 , and net sea – air CO 2 flux over the global oceans. **56**, 554–577 (2009).

759 97. Bakker, D. C. E. *et al.* An update to the Surface Ocean CO₂ Atlas (SOCAT version 2). *Earth Syst. Sci.*
760   *Data* **6**, 69–90 (2014).

761 98. Pfeil, B. *et al.* A uniform, quality controlled Surface Ocean CO2 Atlas (SOCAT). *Earth Syst. Sci.*
762   *Data* **5**, 125–143 (2013).

763 99. Bakker, D. C. E. *et al.* A multi-decade record of high-quality CO2 data in version 3 of the Surface

764   Ocean CO2 Atlas (SOCAT). *Earth Syst. Sci. Data* **8**, 383–413 (2016).

765   100.   Rödenbeck, C. *et al.* Data-based estimates of the ocean carbon sink variability - First results of the
766   Surface Ocean pCO2 Mapping intercomparison (SOCOM). *Biogeosciences* **12**, 7251–7278 (2015).

767   101.   Landschützer, P. *et al.* A neural network-based estimate of the seasonal to inter-annual variability of
768   the Atlantic Ocean carbon sink. *Biogeosciences* **10**, 7793–7815 (2013).

769   102.   Gregor, L., Lebehot, A. D., Kok, S. & Scheel Monteiro, P. M. A comparative assessment of the
770   uncertainties of global surface ocean CO2 estimates using a machine-learning ensemble (CSIR-ML6
771   version 2019a)-Have we hit the wall? *Geosci. Model Dev.* **12**, 5113–5136 (2019).

772   103.   Fay, A. R. *et al.* SeaFlux: Harmonization of air-sea CO2 fluxes from surface pCO2 data products
773   using a standardized approach. *Earth Syst. Sci. Data* **13**, 4693–4710 (2021).

774   104.   Gruber, N. *et al.* Oceanic sources, sinks, and transport of atmospheric CO 2. *Global Biogeochem.*
775   *Cycles* **23**, (2009).

776   105.   Regnier, P., Resplandy, L., Najjar, R. G. & Ciais, P. The land-to-ocean loops of the global carbon
777   cycle. *Nature* **603**, 401–410 (2022).

778   106.   Sarmiento, J. L. & Sundquist, E. T. Revised budget for the oceanic uptake of anthropogenic carbon
779   dioxide. *Nature* **356**, 589–593 (1992).

780   107.   Regnier, P. *et al.* Anthropogenic perturbation of the carbon fluxes from land to ocean. *Nat. Geosci.* **6**,
781   597–607 (2013).

782   108.   Resplandy, L. *et al.* Revision of global carbon fluxes based on a reassessment of oceanic and riverine
783   carbon transport. *Nat. Geosci.* **11**, (2018).

784   109.   Landschützer, P., Ilyina, T. & Lovenduski, N. S. Detecting Regional Modes of Variability in
785   Observation-Based Surface Ocean pCO2. *Geophys. Res. Lett.* **46**, 2670–2679 (2019).

786   110.   Ritter, R. *et al.* Observation-Based Trends of the Southern Ocean Carbon Sink. *Geophys. Res. Lett.*
787   **44**, 12,339-12,348 (2017).

788   111.   Gloege, L. *et al.* Quantifying errors in observationally-based estimates of ocean carbon sink
789   variability. *Global Biogeochem. Cycles* 1–14 (2021). doi:10.1029/2020gb006788

790   112.   Watson, A. J. *et al.* Revised estimates of ocean-atmosphere CO2 flux are consistent with ocean carbon
791   inventory. *Nat. Commun.* **11**, 1–6 (2020).

792   113.   Wanninkhof, R., Asher, W. E., Ho, D. T., Sweeney, C. & Mcgillis, W. R. Advances in Quantifying
793   Air-Sea Gas Exchange and Environmental Forcing*. *Ann. Rev. Mar. Sci.* **1**, 213–244 (2009).

794   114.   DeVries, T., Holzer, M. & Primeau, F. Recent increase in oceanic carbon uptake driven by weaker
795   upper-ocean overturning. *Nature* **542**, 215–218 (2017).

796   115.   Wolter, K. & Timlin, M. S. El Niño/Southern Oscillation behaviour since 1871 as diagnosed in an
797   extended multivariate ENSO index (MEI.ext). *Int. J. Climatol.* **31**, 1074–1087 (2011).

798   116.   Frölicher, T. L. *et al.* Dominance of the Southern Ocean in Anthropogenic Carbon and Heat Uptake in
799   CMIP5 Models. *J. Clim.* **28**, 862–886 (2015).

800   117.   McKinley, G. A., R"odenbeck, C., Gloor, M., Houweling, S. & Heimann, M. Pacific dominance to
801   global air-sea {CO}_2 flux variability: A novel atmospheric inversion agrees with ocean models.
802   *Geophys. Res. Lett.* **31**, (2004).

803   118.   Lenton, A. & Matear, R. J. Role of the Southern Annular Mode (SAM) in Southern Ocean CO 2
804   uptake. *Global Biogeochem. Cycles* **21**, 1–17 (2007).

805   119.   Keppler, L. & Landschützer, P. Regional Wind Variability Modulates the Southern Ocean Carbon
806   Sink. *Sci. Rep.* **9**, 7384 (2019).

807   120.   Le Quéré, C., Takahashi, T., Buitenhuis, E. T., Rödenbeck, C. & Sutherland, S. C. Impact of climate
808   change and variability on the global oceanic sink of CO 2. *Global Biogeochem. Cycles* **24**, n/a-n/a
809   (2010).

810   121.   Feely, R. A., Wanninkhof, R., Takahashi, T. & Tans, P. Influence of El Niño on the equatorial Pacific
811   contribution to atmospheric CO2 accumulation. *Nature* **398**, 597–601 (1999).

812   122.   Ishii, M. *et al.* Air-sea CO2 flux in the Pacific Ocean for the period 1990-2009. *Biogeosciences* **11**,
813   709–734 (2014).

814   123.   McKinley, G. A., Follows, M. J. & Marshall, J. Mechanisms of air-sea CO 2 flux variability in the

815   equatorial Pacific and the North Atlantic. *Global Biogeochem. Cycles* **18**, n/a-n/a (2004).

816   124.   Chatterjee, A. *et al.* Influence of El Niño on atmospheric CO2 over the tropical Pacific Ocean:
817   Findings from NASA's OCO-2 mission. *Science (80-.).* **358**, (2017).

818   125.   Keeling, C. D., Whorf, T. P., Wahlen, M. & v. d. Plicht, J. Interannual extremes in the rate of
819   atmospheric carbon dioxide since 1980. *Nature* **375**, 666–670 (1995).

820   126.   Crisp, D. *et al.* How Well Do We Understand the Land-Ocean-Atmosphere Carbon Cycle? *Rev.*
821   *Geophys.* 1–64 (2022). doi:10.1029/2021rg000736

822   127.   Angert, A., Biraud, S., Bonfils, C., Buermann, W. & Fung, I. CO2 seasonality indicates origins of
823   post-Pinatubo sink. *Geophys. Res. Lett.* **31**, 1999–2002 (2004).

824   128.   Eddebbar, Y. A. *et al.* El Niño-like physical and biogeochemical ocean response to tropical eruptions.
825   *J. Clim.* **32**, 2627–2649 (2019).

826   129.   Marshall, L. R. *et al.* Volcanic effects on climate : recent advances and future avenues. (2022).

827   130.   Thompson, D. W. J. & Solomon, S. Interpretation of recent Southern Hemisphere climate change.
828   *Science* **296**, 895–899 (2002).

829   131.   Hauck, J. *et al.* Seasonally different carbon flux changes in the Southern Ocean in response to the
830   southern annular mode. *Global Biogeochem. Cycles* **27**, 1236–1245 (2013).

831   132.   Lovenduski, N. S., Gruber, N. & Doney, S. C. Toward a mechanistic understanding of the decadal
832   trends in the Southern Ocean carbon sink. *Global Biogeochem. Cycles* **22**, 1–9 (2008).

833   133.   Gillett, N. P. & Thompson, D. W. J. Simulation of recent southern hemisphere climate change.
834   *Science* **302**, 273–5 (2003).

835   134.   Gruber, N., Bates, N. R. & Keeling, C. D. Interannual variability in the {N}orth {A}tlantic carbon
836   sink. *Science (80-.).* **298**, 2374–2378 (2002).

837   135.   Frölicher, T. L., Joos, F., Raible, C. C. & Sarmiento, J. L. Atmospheric CO2 response to volcanic
838   eruptions: The role of ENSO, season, and variability. *Global Biogeochem. Cycles* **27**, 239–251 (2013).

839   136.   DeVries, T. Atmospheric CO 2 and Sea Surface Temperature Variability Cannot Explain Recent
840   Decadal Variability of the Ocean CO 2 Sink . *Geophys. Res. Lett.* **49**, 1–12 (2022).

841   137.   Terhaar, J., Frölicher, T. L. & Joos, F. Observation-constrained estimates of the global ocean carbon
842   sink from Earth system models. *Biogeosciences* **19**, 4431–4457 (2022).

843   138.   Rogelj, J., McCollum, D. L., O'Neill, B. C. & Riahi, K. 2020 emissions levels required to limit
844   warming to below 2 °C. *Nat. Clim. Chang.* **3**, 405–412 (2012).

845   139.   Keller, D. P. *et al.* The Effects of Carbon Dioxide Removal on the Carbon Cycle. *Curr. Clim. Chang.*
846   *Reports* **4**, 250–265 (2018).

847   140.   Smith, P. *et al.* Biophysical and economic limits to negative CO2 emissions. *Nat. Clim. Chang.* **6**, 42–
848   50 (2016).

849   141.   National Academies of Sciences. *A Research Strategy for Ocean-based Carbon Dioxide Removal and*
850   *Sequestration*. (National Academies Press, 2022). doi:10.17226/26278

851   142.   Aricò, S. *et al. Integrated Ocean Carbon Research: A Summary of Ocean Carbon Research, and*
852   *Vision of Coordinated Ocean Carbon Research and Observations for the Next Decade*. (2021).
853   doi:10.25607/h0gj-pq41

854   143.   Gruber, N., Boyd, P. W., Frölicher, T. L. & Vogt, M. Biogeochemical extremes and compound events
855   in the ocean. *Nature* **600**, 395–407 (2021).

856   144.   Djeutchouang, L. M., Chang, N., Gregor, L., Vichi, M. & Monteiro, P. M. S. The sensitivity of p CO
857   2 reconstructions to sampling scales across a Southern Ocean sub-domain: a semi-idealized ocean
858   sampling simulation approach. *Biogeosciences* **19**, 4171–4195 (2022).

859   145.   Majkut, J. D. *et al.* An observing system simulation for Southern Ocean carbon dioxide uptake.
860   *Philos. Trans. R. Soc. A Math. Phys. Eng. Sci.* **372**, 20130046–20130046 (2014).

861   146.   Claustre, H., Johnson, K. S. & Takeshita, Y. Observing the Global Ocean with Biogeochemical-Argo.
862   *Ann. Rev. Mar. Sci.* **12**, 23–48 (2020).

863   147.   Gray, A. R. *et al.* Autonomous Biogeochemical Floats Detect Significant Carbon Dioxide Outgassing
864   in the High-Latitude Southern Ocean. *Geophys. Res. Lett.* **45**, 9049–9057 (2018).

865   148.   Bushinsky, S. M. *et al.* Reassessing Southern Ocean air-sea CO2 flux estimates with the addition of

866   biogeochemical float observations. *Global Biogeochem. Cycles* **33**, 1–19 (2019).

867   149.   Verdy, A. & Mazloff, M. R. A data assimilating model for estimating Southern Ocean
868   biogeochemistry. *J. Geophys. Res. Ocean.* **122**, 6968–6988 (2017).

869   150.   Carroll, D. *et al.* Attribution of Space-Time Variability in Global-Ocean Dissolved Inorganic Carbon.
870   *Global Biogeochem. Cycles* **36**, 1–24 (2022).

871   151.   Bennington, V., Gloege, L. & McKinley, G. A. Variability in the Global Ocean Carbon Sink From
872   1959 to 2020 by Correcting Models With Observations. *Geophys. Res. Lett.* **49**, (2022).

873   152.   Lacroix, F., Ilyina, T. & Hartmann, J. Oceanic CO2 outgassing and biological production hotspots
874   induced by pre-industrial river loads of nutrients and carbon in a global modeling approach.
875   *Biogeosciences* **17**, 55–88 (2020).

876   153.   Kwon, E. Y. *et al.* Stable Carbon Isotopes Suggest Large Terrestrial Carbon Inputs to the Global
877   Ocean. *Global Biogeochem. Cycles* 1–25 (2021). doi:10.1029/2020gb006684

878   154.   GESAMP. *High level review of a wide range of proposed marine geoengineering techniques.*
879   *GESAMP Reports and Studies* (2019).

880   155.   Dlugokencky, E. & Tans, P. Trends in atmospheric carbon dioxide. *National Oceanic&Atmospheric*
881   *Administration; Global Monitoring Laboratory (NOAA/GML)* (2022). Available at:
882   http://gml.noaa.gov/ccgg/trends/. (Accessed: 15th July 2015)

883   156.   Kroeker, K. J. *et al.* Impacts of ocean acidification on marine organisms: quantifying sensitivities and
884   interaction with warming. *Glob. Chang. Biol.* **19**, 1884–1896 (2013).

885   157.   Landschützer, P., Gruber, N., Bakker, D. C. E., Stemmler, I. & Six, K. D. Strengthening seasonal
886   marine CO2 variations due to increasing atmospheric CO2. *Nat. Clim. Chang.* **8**, 146–150 (2018).

887   158.   Hauck, J. & Völker, C. Rising atmospheric CO 2 leads to large impact of biology on Southern Ocean
888   CO2 uptake via changes of the Revelle factor. *Geophys. Res. Lett.* **42**, 1459–1464 (2015).

889   159.   Gruber, N. & Sarmiento, J. L. Large-scale biogeochemical/physical interactions in elemental cycles.
890   in *THE SEA: Biological-Physical Interactions in the Oceans* (eds. Robinson, A. R., McCarthy, J. J. &
891   Rothschild, B. J.) **12**, 337–399 (John Wiley and Sons, 2002).

892

893

894

895

906

907 **Author contributions**
908 N.G. led the conceptual design and the implementation and also wrote the first draft. J.-D.M. was responsible
909 for the generation of Fig 1 and Table 1. P.L. generated Fig 2, L.G. generated Figs 3 and 4, and N.G. drew Fig
910 5. All authors contributed to the outline, discussed the content and conclusions and provided input to the
911 manuscript during all drafting stages.
912

913 **Competing interests**
914 The authors declare not competing interests.
915

916 **Peer review information**
917 *Nature Reviews Earth & Environment* thanks [Referee#1 name], [Referee#2 name] and the other,
918 anonymous, reviewer(s) for their contribution to the peer review of this work.

919 **Publisher's note**
920 Springer Nature remains neutral with regard to jurisdictional claims in published maps and institutional
921 affiliations.

922 **Supplementary information**
923 Supplementary information is available for this paper at https://doi.org/10.1038/s415XX-XXX-XXXX-X
924
925

926
927   **Tables**

928
929
930
931

932   TABLE 1.

933

934   OCEAN CO_2 UPTAKE FROM 1990-2019.

935

Method	Reference	Components[*]	1990–1999 (Pg C yr^{-1})	2000–2009 (Pg C yr^{-1})	2010–2019 (Pg C yr^{-1})
		ATMOSPHERIC CO_2			
Change in atmospheric CO_2 (ppm)	[155]		15.0	18.7	23.6
		OCEAN CO_2 UPTAKE			
Change in interior accumulation of ant. CO_2 (†)	[4]	$F_{ant}^{ss} + F_{ant}^{ns}$	-2.1±0.2	-2.6±0.3	-3.3±0.3
Ocean inverse model (Green's function)	[3]	F_{ant}^{ss}	-2.0±0.6	-2.3±0.6	NA
Ocean inverse model (Adjoint)	[136]	F_{ant}^{ss}	-2.2±0.1	-2.5±0.1	-2.9±0.2
Ocean inverse model (Adjoint) (§)	[136]	$F_{ant}^{ss}+ F_{nat}^{ns}$	-2.0±0.1	-2.3±0.1	-2.7±0.2
Ocean forward models	[25]	$F_{ant}^{ss} + F_{ant}^{ns} + F_{nat}^{ns}$	-2.0±0.2	-2.1±0.3	-2.5±0.3
Surface ocean pCO$_2$ products (#)	[103]	$F_{ant}^{ss} + F_{ant}^{ns} + F_{nat}^{ns}$	-2.1±0.4	-2.3±0.2	-3.1±0.2

936

937 (*) F_{ant}^{ss} : steady-state uptake flux component of anthropogenic CO_2 (part driven solely by the increase in atmospheric

938 CO_2); F_{ant}^{ns}: non-steady-state uptake component of anthropogenic CO_2 (part driven by variations in ocean circulation and

939 other physical drivers); F_{nat}^{ns}: non-steady-state exchange component of natural CO_2 (part driven by variations in ocean

940 circulation and other physical drivers). (see Box 1)

941 (†) scaled using $\beta = 1.39$ Pg C/ppm CO_2 and the change in atmospheric pCO$_2$ indicated in the first line.

942 (§) Non-steady component is only due to SST variability (warming).

943 (#) Adjusted for the steady-state outgassing of river derived CO_2.

944

945

946   Box 1 | **Key concepts in ocean carbon sink investigations**

947

948   [bH1] Natural versus anthropogenic CO_2

949   A key concept aiding the interpretation of the ocean carbon sink has been the separation of the air-sea CO_2

950   fluxes and the changes in the ocean interior storage of DIC into natural and anthropogenic CO_2 components[38].

951   The natural CO_2 component (C_{nat}) is the part of the ocean's DIC pool that existed in pre-industrial times. This

952   pool is involved in many processes, namely air-sea gas exchange, uptake and release by the biological pumps,

953   interactions with and loss to the sediments, and input by rivers (Box Figure 1a). The anthropogenic component

954   (C_{ant}) represents the perturbation to the DIC pool, driven by the anthropogenically-driven increases in

955   atmospheric CO_2. It is substantially smaller than the natural DIC pool (Box Figure 1b).

956   An important assumption that has simplified analysis is that the anthropogenic CO_2 component does not interact

957   with the natural CO_2 component[38]. Therefore, the only processes of importance for anthropogenic CO_2 are the

958   uptake from the atmosphere via air-sea gas exchange and the subsequent transport to depth (Box Figure 1a).

959   The assumption about the lack of interaction between the two pools is generally well met, but there are some

960   exceptions. For example, the acidification induced by the oceanic accumulation of anthropogenic CO_2 can

961   affect ocean biology[156] and also has been shown to modify the flux of natural CO_2[157,158].
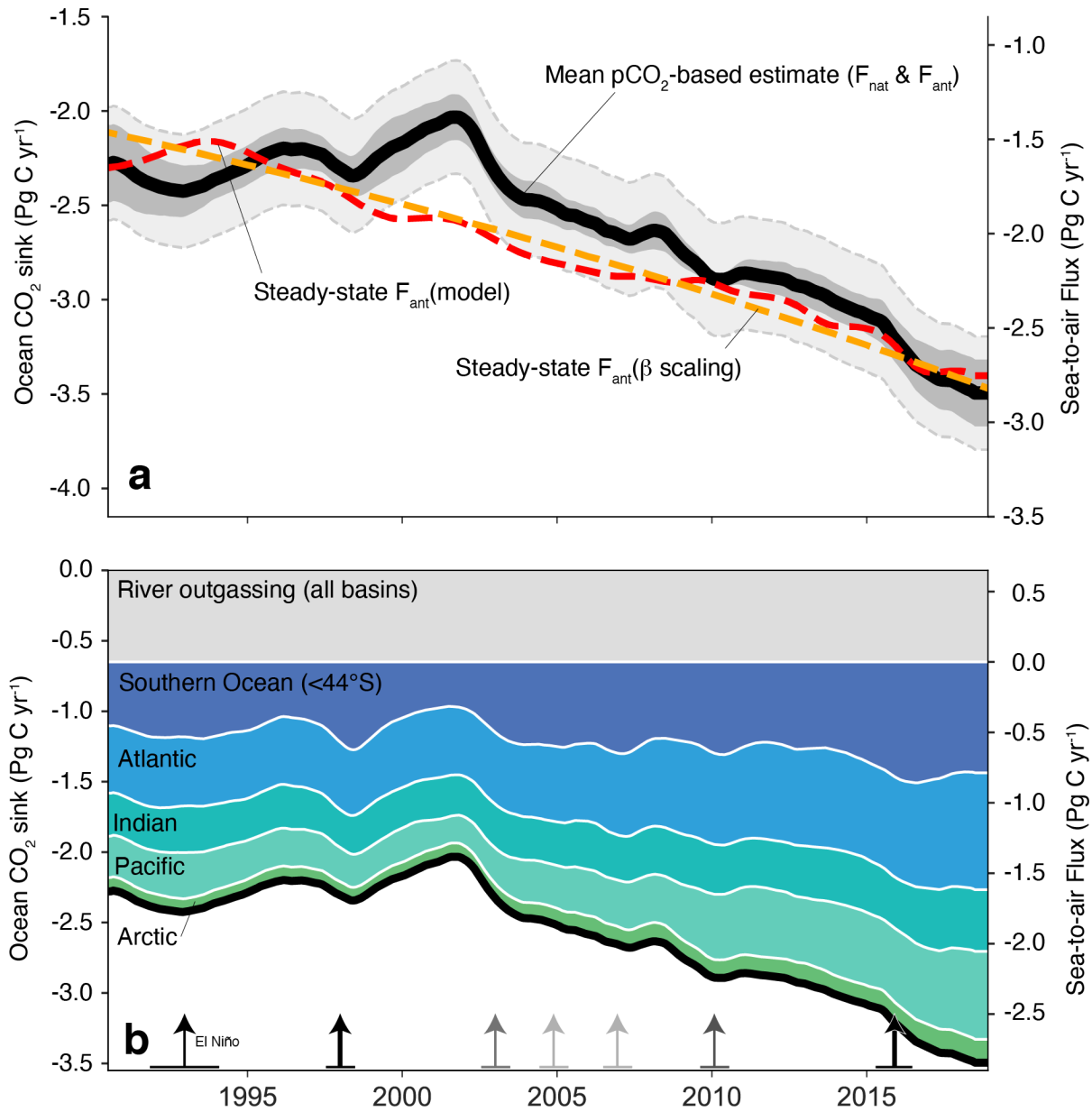
962   [bH1] The steady state ocean

963   The second key concept is steady-state, which is reached if climate forcing remains constant for long enough

964   for ocean circulation and ocean biology to become unchanging with time. In this situation, natural CO_2 fluxes

965   across the air-sea interface balance to zero on a global scale[104], with the exception of steady-state outgassing of

966   river-derived CO_2[105]. Biological fluxes are also balanced over the annual cycle. The only variations in time

967   come from the steady-state uptake of anthropogenic CO_2 (Box Figure 1c, e). If climate is permitted to vary,

968   leading to a non-steady-state situation, both natural and anthropogenic CO_2 components are affected, leading

969   to additional fluxes and changes in storage (Box Figure 1 d,f). The non-steady-state component of natural CO_2

970   emerges from a situation where climate is varying, but where atmospheric CO_2 is kept at its preindustrial level.

971   The difference between this situation with one where atmospheric CO_2 is permitted to increase gives the non-

972   steady-state component of anthropogenic CO_2 (Box Figure 1, c-f).

973

974

975

976

977 **Figures**
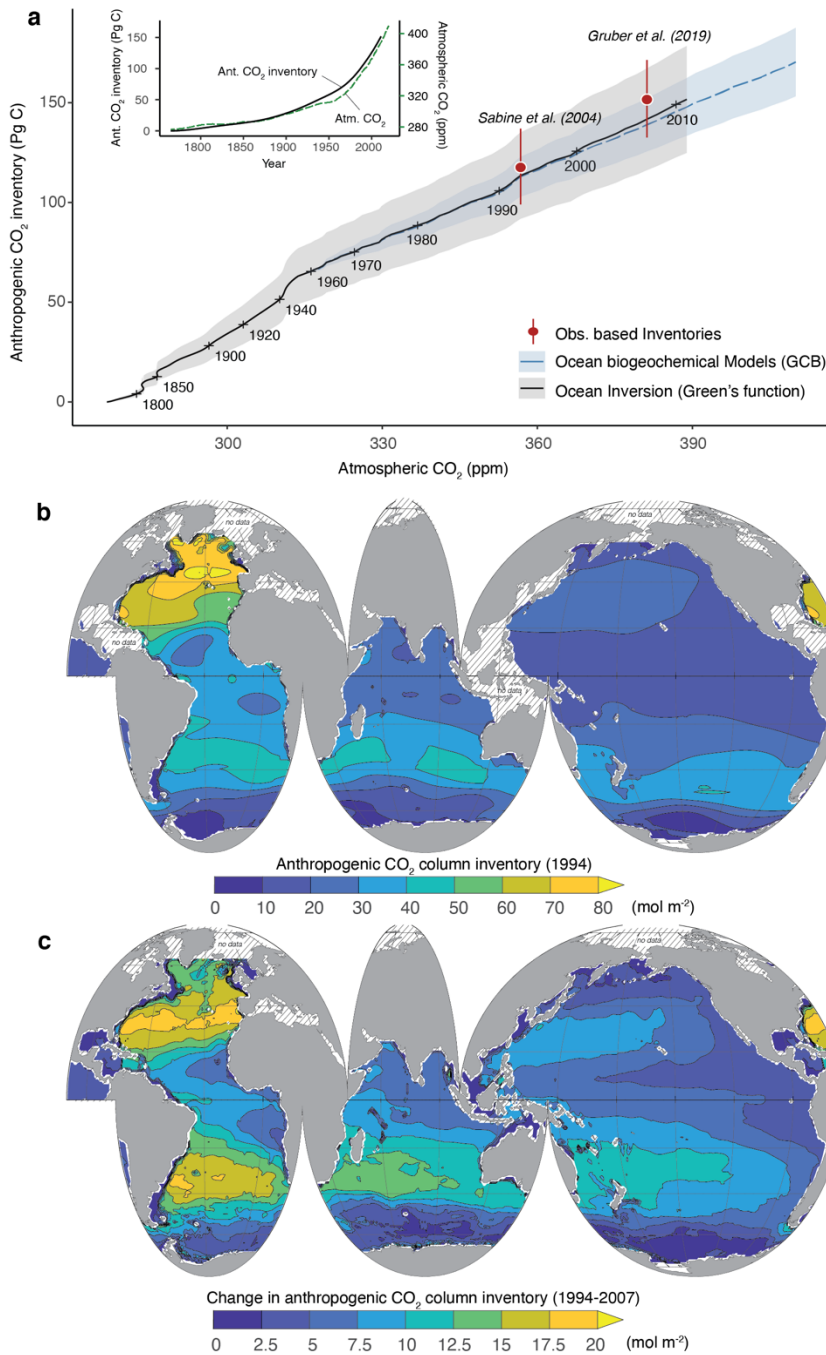
978
979 Fig 1. **Ocean uptake and storage of anthropogenic CO₂. a** | Temporal progression of the total ocean
980 inventory of anthropogenic CO_2 as a function of the atmospheric CO_2 content. Results are from an ocean
981 inverse model[3] (black line and grey shaded band indicating uncertainty) spanning the period from 1765 until
982 2010, the ocean biogeochemical model results used in the Global Carbon Budget[25] (blue line for the mean
983 and blue shaded band representing the standard deviation), and two observation based estimates of the ocean
984 interior accumulation of anthropogenic CO_2 [2,4] for 1994 and 2007. The inset shows the time history of
985 atmospheric CO_2 and the ocean CO_2 uptake[3]. The bands represent the cumulative uncertainty from the start of
986 the respective estimate. The nearly linear scaling of the ocean uptake with the atmospheric CO_2 content is

987   particularly evident after 1959. The ocean biogeochemical model results shown here include also the non-
988   steady-state, component of natural CO_2 (climate variability). **b** | Column inventory of anthropogenic CO_2 in
989   mol m^{-2} for the year 1994 estimated using the ΔC^* back-calculation method [2]. Strong regional patterning of
990   the accumulation of anthropogenic CO_2 in the ocean was driven by regional differences in ocean circulation
991   and mixing. **c** | Change in the water column inventory between 1994 and 2007 estimated by the eMLR(C*)
992   method [4]. In b and c, the hatching indicates regions that were not mapped.
993

994
995
996 Fig 2. **Climatological-mean sea-to-air CO_2 flux**. Multi-product mean estimate based on the six pCO_2-based
997 estimates contained in the SeaFlux product[103]. The mean for the period 1990 through 2020 is depicted,
998 representing the sum of natural, anthropogenic, and steady-state riverine flux components for the nominal
999 year of 2005. The global ocean is characterized by regions of strong sources and sinks of CO_2, reflecting
1000 primarily the exchange of natural CO_2 across the air-sea interface. This flux is regionally modified by the
1001 uptake flux of anthropogenic CO_2. The latter integrates globally to an uptake flux of about 2.6 Pg C yr^{-1} for
1002 this nominal year. The total CO_2 flux also includes an outgassing flux of about 0.65±0.30 Pg C yr^{-1}, reflecting
1003 the steady-state outgassing of natural CO_2 associated with the imbalance between river input and burial[105].
1004

1005
1006
1007 Fig 3. **Temporal evolution of the global ocean CO$_2$ sink a** | Global ocean CO$_2$
1008 observation based products contained in SeaFlux [103]. The estimated net sea-to-air fluxes were adjusted by the
1009 steady-state river outgassing flux of 0.65 Pg C yr^{-1} [105] to obtain the ocean CO$_2$ sink flux that is of relevance
1010 for balancing the global sources and sinks of CO$_2$ (the natural flux, F$_{nat}$, plus the anthropogenic flux, F$_{ant}$). The
1011 solid black line indicates the mean estimate with the dark grey area representing the standard error across the
1012 6 products. The dashed grey lines indicate the uncertainty of the ocean sink and include the uncertainty of
1013 ±0.30 Pg C yr^{-1} associated with the river outgassing flux[105]. The dashed red line represents the steady-state
1014 uptake of anthropogenic CO$_2$ estimated from a global ocean model (CESM-ETHZ[25]). The dashed orange line
1015 represents the expected steady-state uptake of anthropogenic CO$_2$ estimated from the sensitivity β (left axis).
1016 **b** | Contribution of individual ocean basins (north of 44°S) to the global ocean CO$_2$ sink based on the
1017 ensemble mean of the SeaFlux products. The grey band represents the steady-state oceanic outgassing of
1018 river-derived CO$_2$. It was not allocated to individual basins. El Niño related variations in the Pacific basin are

1019   represented by arrows, with the grey shading indicating strength (darker arrows for stronger events).The

1020   global ocean carbon sink varies substantially in time around the long-term trend given by the steady-state

1021   uptake of anthropogenic CO_2 with a period of stagnant uptake in the 1990s followed by a period of faster than

1022   expected growth of the ocean carbon sink after the turn of the millennium.

1023
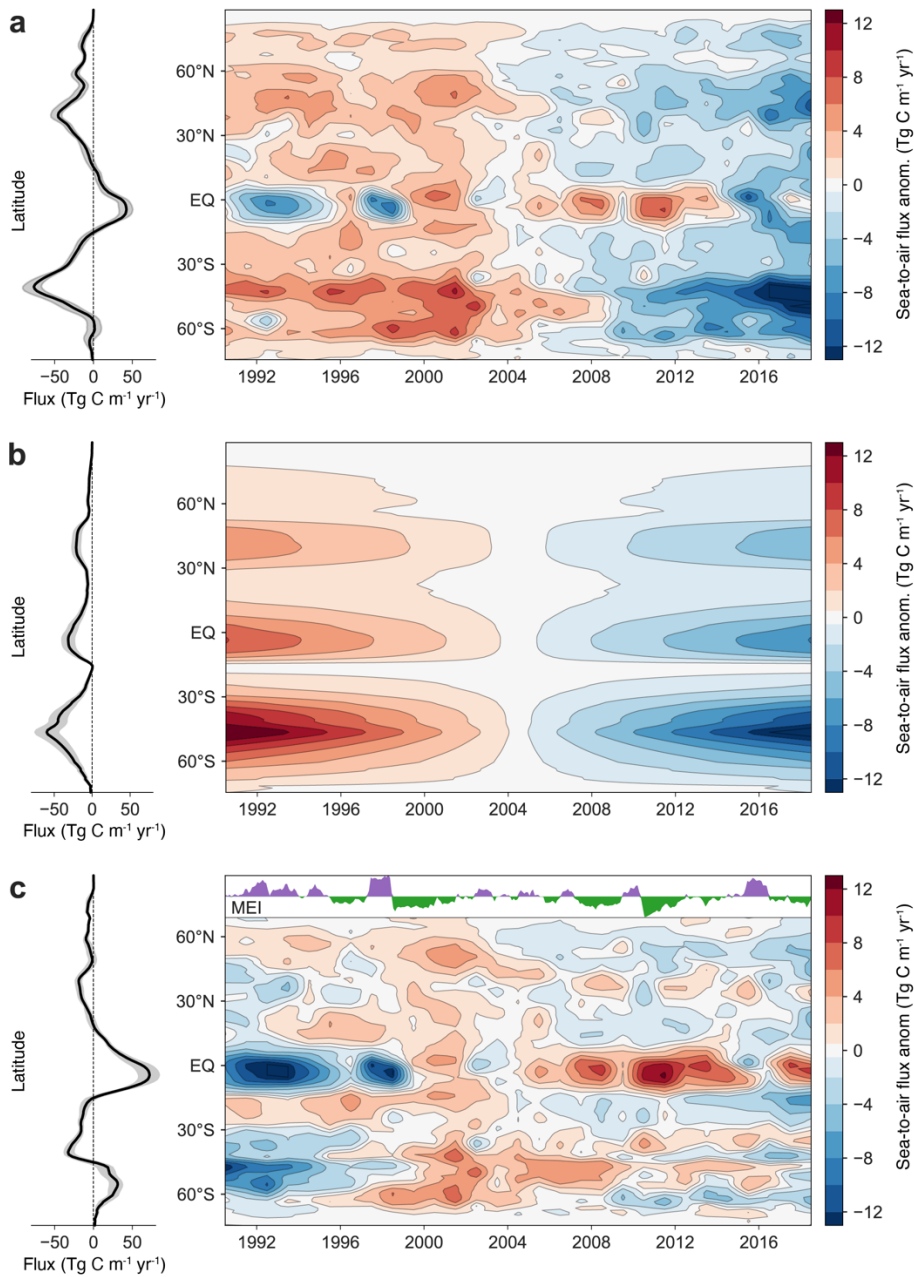
1024
1025
1026 Fig 4. **Zonally integrated anomalous CO$_2$ fluxes and its components. a** | Hovmoeller diagram of the
1027 annual mean, zonal mean anomalies of the total air-sea CO$_2$ fluxes as a function of time and latitude (right
1028 panels) together with the zonal mean (left panels). The anomalies were computed by subtracting the long-
1029 term mean flux from the annual mean flux for a given year using the ensemble mean data from the SeaFlux
1030 product[103]. The ribbon in the left panels shows the range of the integrated fluxes relative to the zonal mean.
1031 The zonal mean dominates compared to the interannual variability. **b** | The same as a, but for the anomalous
1032 air-sea fluxes of the steady-state component of anthropogenic CO$_2$. This estimate was obtained by scaling the
1033 ocean inversion-based estimate [72] for 1995 with a β of 1.4 Pg C (ppm CO$_2$)$^{-1}$. The anomalies were then
1034 obtained by subtracting the long-term mean flux. **c** | The same as a, but for the anomalous air-sea fluxes of the
1035 non-steady-state component of CO$_2$, obtained by subtracting b from a. There is strong interannual variability
1036 of the air-sea fluxes in the tropics, largely associated with El Niño/Southern Oscillation (ENSO) dynamics as

34

1037   indicated by the timeseries of the multivariate ENSO index (MEI)[115] in panel c, and the strong decadal

1038   variations in the Southern Ocean, largely driven by the non-steady state components.

1039
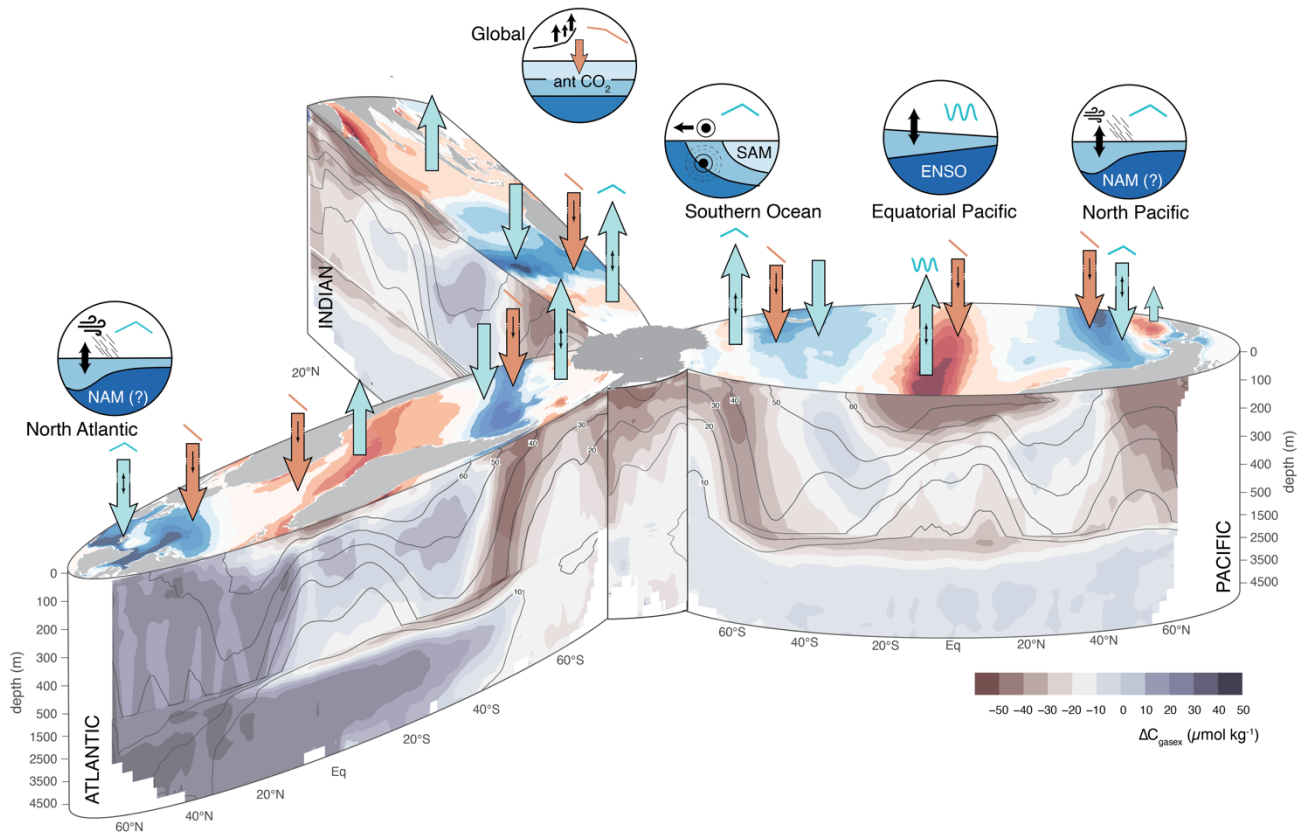
Fig 5. **Interannual to decadal variability in the ocean carbon sink**. The global ocean sources and sinks of CO_2 are shown along the surface ocean. The ocean interior distribution of the gas-exchange component of natural CO_2 [104,159] (colors) and of the total amount of anthropogenic CO_2 for 2007 [2,4] (isolines) are shown along the depth profile. The hotspots for interannual and decadal variability are noted by the insets. Gradients in the gas-exchange component of natural CO_2 reflects the addition or removal of natural CO_2 through air-sea exchange at the surface. The turquoise arrows indicate the sea-to-air fluxes of natural CO_2 including the type and direction of variability (hat: decadal variability, waves: interannual variability). The reddish arrows indicate the oceanic uptake of anthropogenic CO_2which is increasing everywhere (straight line). Not shown as arrows is the outgassing flux of the river-derived natural CO_2. The icons relate the variations in the dominant regions of variability (tropical Pacific, and the higher latitudes) to the underlying processes, such as El Niño-Southern Oscillation (ENSO) in the tropical Pacific, and the high latitude modes of variability, especially the Southern Annular Mode (SAM) and the Northern Annular Mode (NAM). Changes in atmospheric CO_2 growth rates affect the global uptake of anthropogenic CO_2.

1057
1058   **Glossary**

1059
1060   AIR-SEA GAS EXCHANGE
1061   A diffusion-driven process governing the transfer of gases across the air-sea interface, driven by the
1062   concentration gradient of the gas across the interface and controlled by the level of turbulence at the interface.
1063
1064   BUFFER FACTOR (REVELLE FACTOR)
1065   The ocean's buffer factor describes how well seawater is able to buffer an increase in surface ocean CO_2
1066   (pCO_2) and is thus crucial for determining the amount of anthropogenic CO_2 the surface ocean can hold.
1067
1068   CARBON, DISSOLVED INORGANIC (DIC)
1069   Dissolved inorganic carbon (DIC) is the sum of all dissolved inorganic carbon species in the seawater, and
1070   includes dissolved CO_2 (CO_2^{aq}), carbonic acid (H_2CO_3), bicarbonate (HCO_3^-), and carbonate (CO_3^{2-}).
1071
1072
1073 CO_2, OCEANIC PARTIAL PRESSURE OF (pCO_2)
1074   The oceanic partial pressure of CO_2, pCO_2^{oc} or often just pCO_2, is the partial pressure of CO_2 measured in the
1075   air in equilibrium with the water parcel under consideration at one atmosphere total pressure and at the in-situ
1076   temperature of the water parcel.
1077
1078
1079   EL NIÑO - SOUTHERN OSCILLATION (ENSO)
1080   The El Niño-Southern Oscillation is a quasi-periodic oscillation of the coupled ocean-atmosphere system
1081   with the majority of the action being focused on the eastern tropical Pacific; it is globally the dominant mode
1082   of climate variability.
1083
1084   INVERSE MODELS
1085   Inverse models describe a class of models that fuse observations and models in order to improve our
1086   quantitative understanding of a set of processes.
1087
1088   FORCING, INTERNAL AND EXTERNAL
1089   Processes leading to changes in the ocean carbon sink: Internal forcing is primarily associated with (internally
1090   generated) weather and climate variations, while external forcing is driven by processes external to the
1091   climate system, such as volcanic eruptions.
1092
1093   FORWARD MODELS
1094   Forward models, such as those used for the Global Carbon Budget, are a class models that start from initial
1095   conditions and solve the governing balance equations by time-integrating them forward using a set of
1096   provided boundary conditions.
1097
1098   OCEAN ACIDIFICATION
1099   Change in the ocean's seawater chemistry (pH, $[CO_3^{2-}]$, $CaCO_3$ saturation state, etc) as a consequence of the
1100   oceanic uptake of anthropogenic CO_2.
1101

1102
1103 OCEAN BIOGEOCHEMICAL MODELS
1104 Ocean biogeochemical models are a class of ocean models where the most important biogeochemical
1105 processes are explicitly represented, namely air-sea gas exchange, chemical speciation, and biological
1106 processes.